創発的研究支援事業
Fusion Oriented REsearch for disruptive Science and Technology

KEK IPNS

Theoretical cosmology

Yuko Urakawa (KEK IPNS)

ICFA seminar, Nov 6th 2026

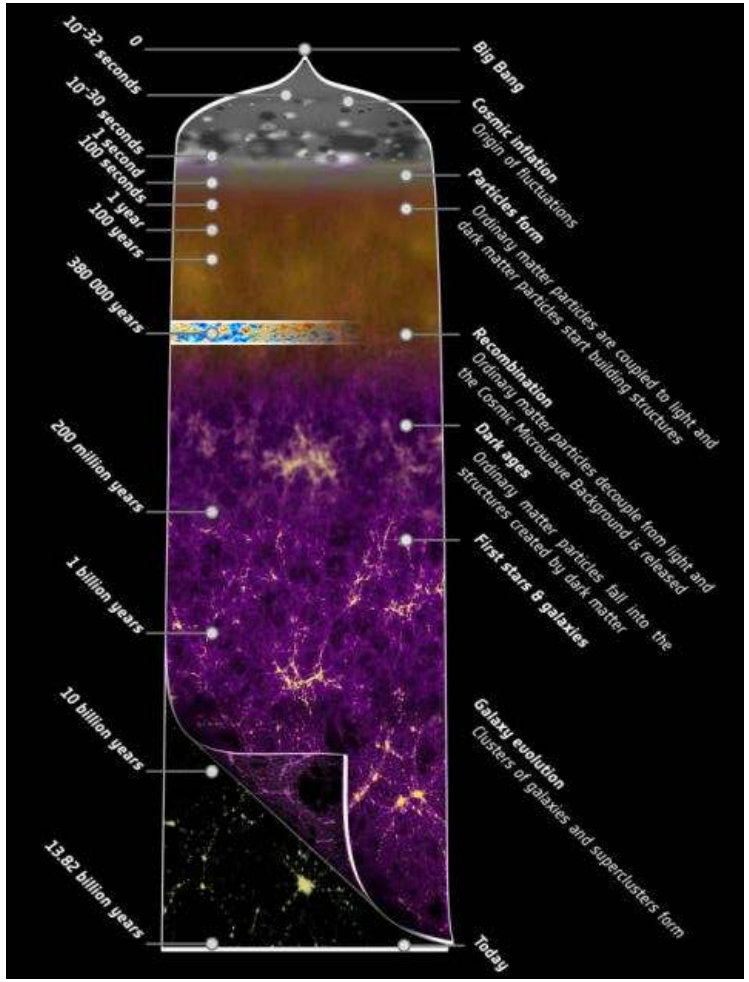
Outline

We know the gross picture of the cosmic history but the microphysics/origins remain unknown.

1) Initial conditions of Big Bang cosmology and inflation

2) Structure formation and dark matter

3) Accelerated expansion and dark energy



Cosmic inflation

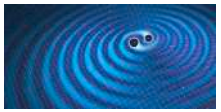
Gravity + ϕ (inflaton)

ζ

scalar potential
~ energy density



gws



massless (from Diff)

Massless fields during inflation ~ de Sitter sp. w/time trans. sym.

$d\langle\phi_I^2\rangle/d\ln k \sim k^3 P_\phi(k) \equiv \Delta_\phi$ ~ const approx. scale inv. $n_s \sim 1$

Deviation from de Sitter

1) Deviation from exact scale-invariance (Harrison-Zeldvich)

Time trans. sym → scale inv. $n_s = 1$ ~8σ exclusion (PLANCK 18)

2) Non-zero tensor to scalar $r = \Delta_{\rm gw}/\Delta_\zeta$

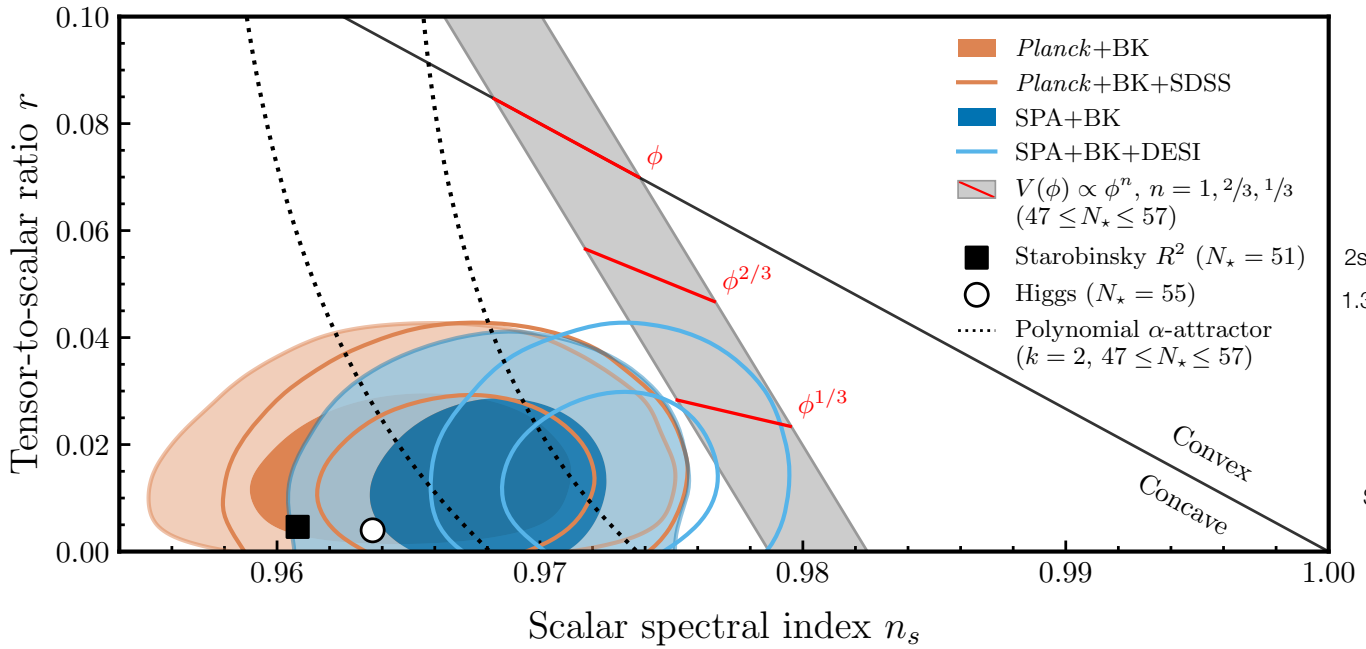
ζ ~ time clock → becomes ill-defined w/time trans. sym.

(n_s, r) plot: Deviations from dS

see Akito's talk

Balkenhol et al. (26)

2) $r \simeq 16\varepsilon$



$\varepsilon \propto (V_\phi/V)^2$

under SR approx.

$\eta \propto V_{\phi\phi}/V$

2sigma (SPA+BK)

1.3sigma (SPA+BK) for a given $N_\star$

BK: BICEP + Keck

SPA: SPT + PLANCK +ACT

1) Deviation from exact scale inv. $\quad n_s - 1 \simeq -6\varepsilon + 2\eta$

- $n_s - 1 < 0$ (Red-tilt spec.) $\longrightarrow$ $\eta_V \propto V_{\phi\phi} < 0$ (Concave)

+ non-detection of r

- $r < 0.034$,(95%) $n_s = 0.9682 \pm 0.0032$ (68%)

N.B. - via $N_\star$, it also depends on microphysics e.g., during reheating.

- correlation w/Ω_m Ferreira et al. (25) 2507.12459

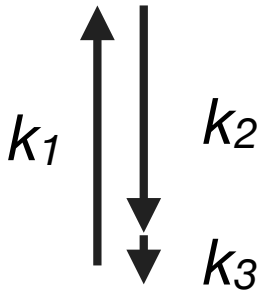
Non Gaussianity

- Non-linear interactions generate (intrinsic) higher point fns.

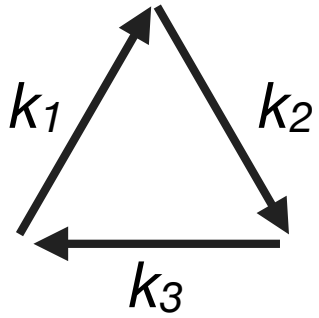
- Different interactions can generate different configurations

- bi-spectrum templates

Local



Equilateral



Orthogonal

and so on…

# of light species

$$f_{\rm NL}^{\rm local} = -0.1 \pm 5.0$$

Derivative forms

$$f_{\rm NL}^{\rm eq} = 6 \pm 46$$

$$f_{\rm NL}^{\rm ortho} = -8 \pm 21$$

Jung et al (PLANCK DR4, 2504.00884)

Lyth bound and distance conjecture

Lyth bound

Lyth (96)

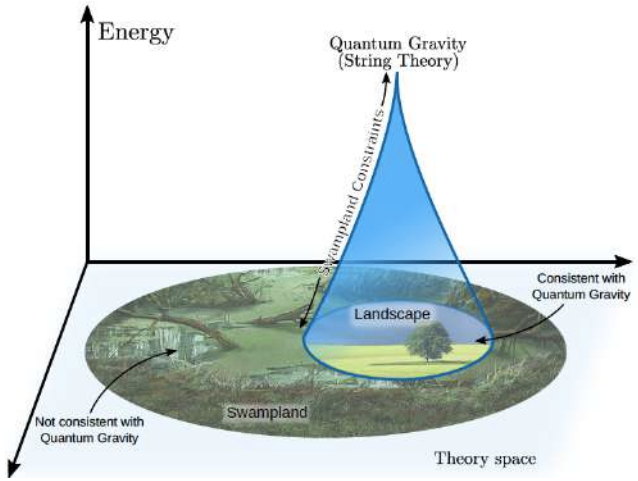
T/S ratio r is related to the change of field value ϕ (deviation from dS)

$$\frac{\Delta\phi}{M_{\rm pl}} \sim \sqrt{\frac{r}{0.002}} \times \frac{\Delta N}{60}$$

Simons Observatory (SO) $\sigma(r) \sim 10^{-3}$ *see Akito's talk*

SO can tell the amount of excursion, e.g, $\Delta\phi > M_{\rm pl}$ or $\Delta\phi < M_{\rm pl}$ (under extra assumptions)

Swampland and Distance conjecture



Ooguri–Vafa(06)

for $\Delta\phi > M_{\rm pl}$, a tower of state is conjectured to become exponentially light.

→ potentially limiting low-energy EFT

figure from *Beest et al. (21)*

Cosmological colliders

Heavy particles → **Imprints** → **Detector**

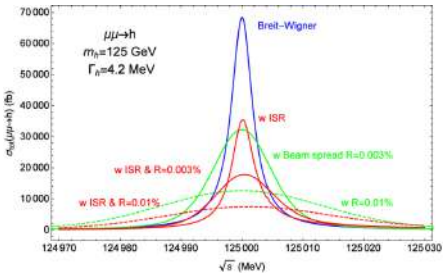
Collider experiment

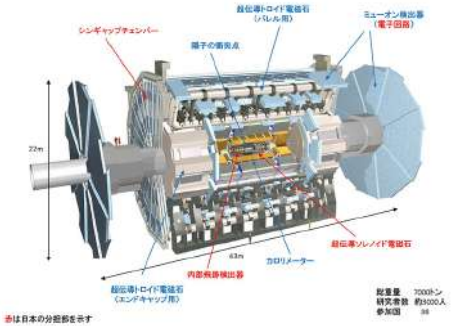
Collision of particles



eg. LHC (~10^3GeV)

Resonance-like structure in collider signals

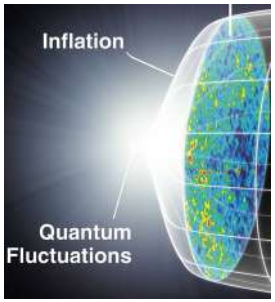




eg. ATLAS

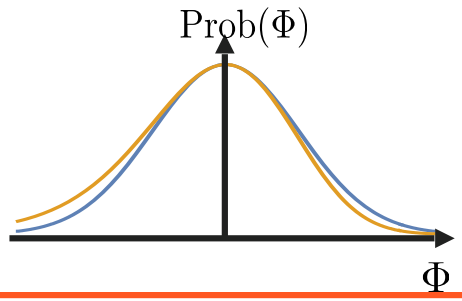
Cosmology

Heavy particles during inflation (~10^{13}GeV)

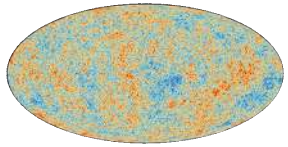


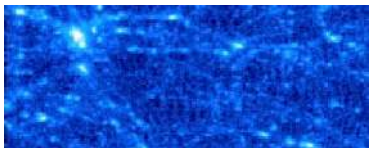
Statistical properties of primordial perturbations

e.g. Deviation from Gaussian



Cosmological observables



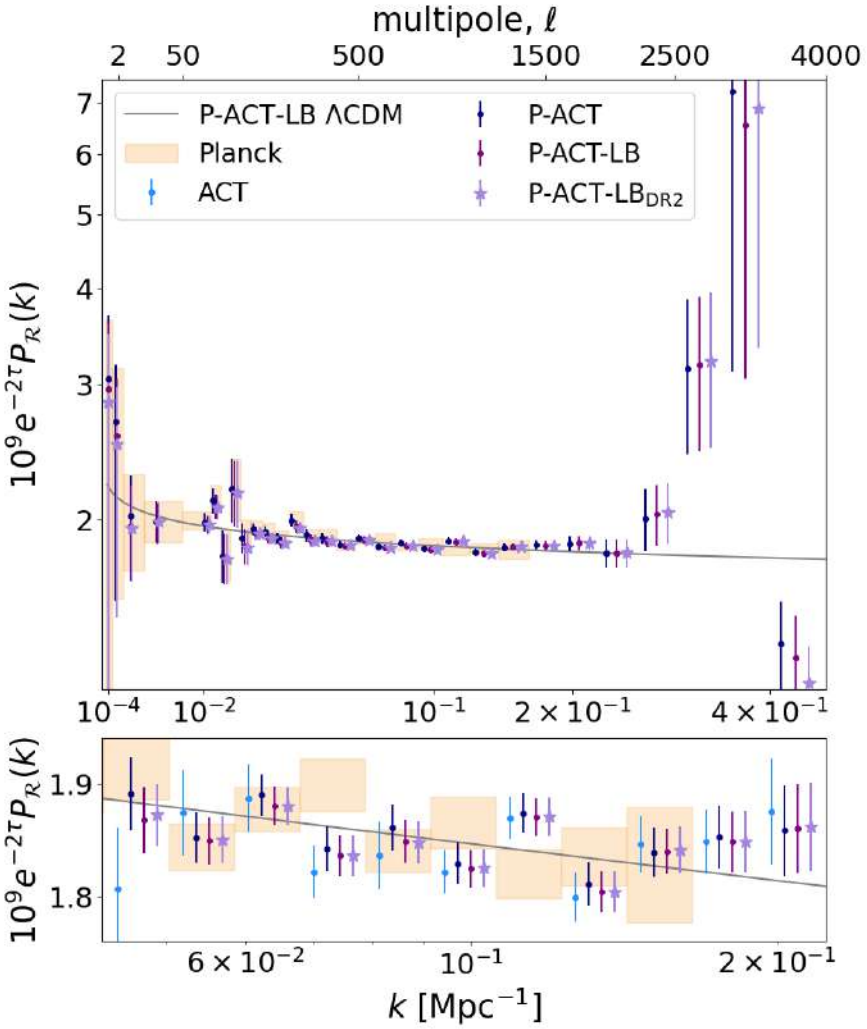


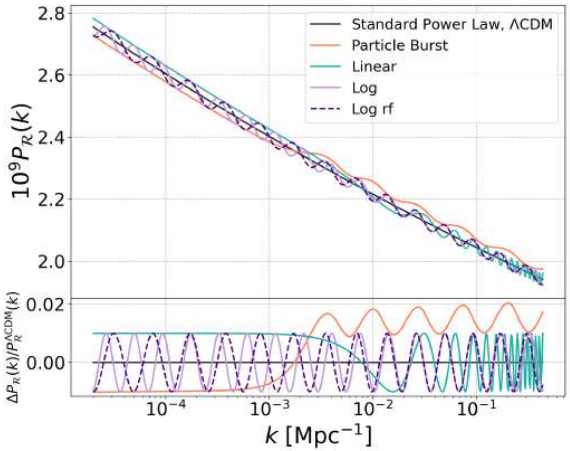
Statistical properties of primordial map → New probe of HEP beyond accelerator exp.

Particle creation during inflation ?

Nerval, Hlozek, Jense, Bond (26)

binned reconstruction of PPS (68%CL)





Models

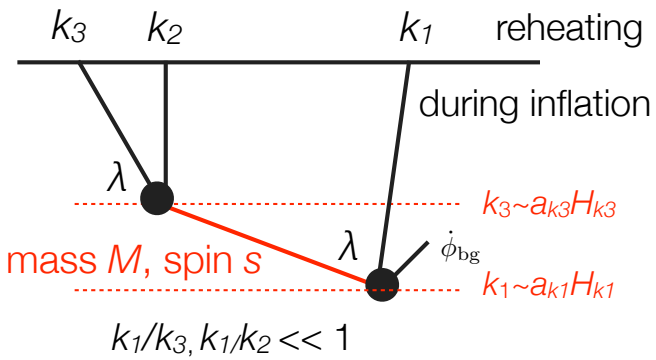
1) General oscillation

e.g.,Axion monodromy inflation

2) Burst particle production

Marginal improvements in fits yet, but no clear preference over ΛCDM in Bayesian evidence.

Imprint of heavy particles on non-Gaussianity



$$\sim \lambda^2 \dot{\phi}_{\rm bg} e^{-M/T_{\rm H}} \left(\frac{k_1}{k_3}\right)^{\Delta} (\hat{\mathbf{k}}_1 \cdot \hat{\mathbf{k}}_3)^s \mathcal{P}(k_1)\mathcal{P}(k_3)$$

Arkani-Hamed & Maldacena (15)

mass (oscillation due to interference)

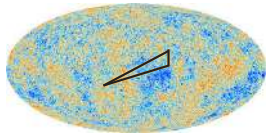
spin

$\mathcal{P}(k)$:power spectrum

Need to combine all possible data

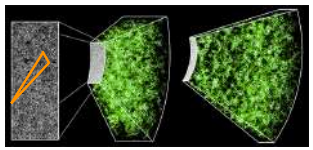
1) Cosmic microwave background <δTδTδT>

PLANCK18, Bartolo et al. (17), Franciolini et al. (18), Bordin & Cabass (19), Sohn et al. (23, 24)



2) Galaxy number count <δn δn δn>

Moradinezhad et al (18[1],18[2]),....

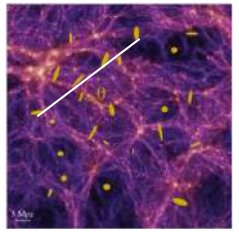


3) Two point galaxy statistics

spin s=0 → <δn δn> Dalal (07),.....

spin s=2 → <γ γ> Schmidt et al (15, 16), Kogai,...., Y,U. (18),....

spin s>4 → <γ$_l$ γ$_l$> γ$_l$:l-th mom. Kogai,...., Y,U. (21)



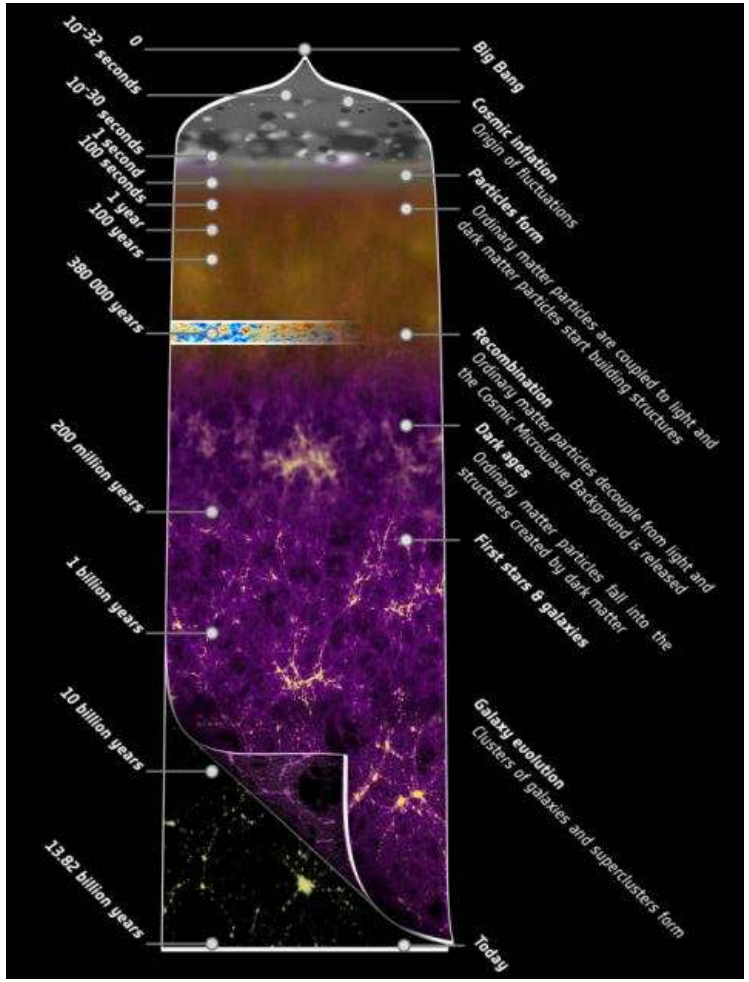
Outline

We know the gross picture of the cosmic history but the microphysics/origins remain unknown.

1) Initial conditions of Big Bang cosmology and inflation

2) Structure formation and dark matter

3) Accelerated expansion and dark energy



Dark matter

We need either of

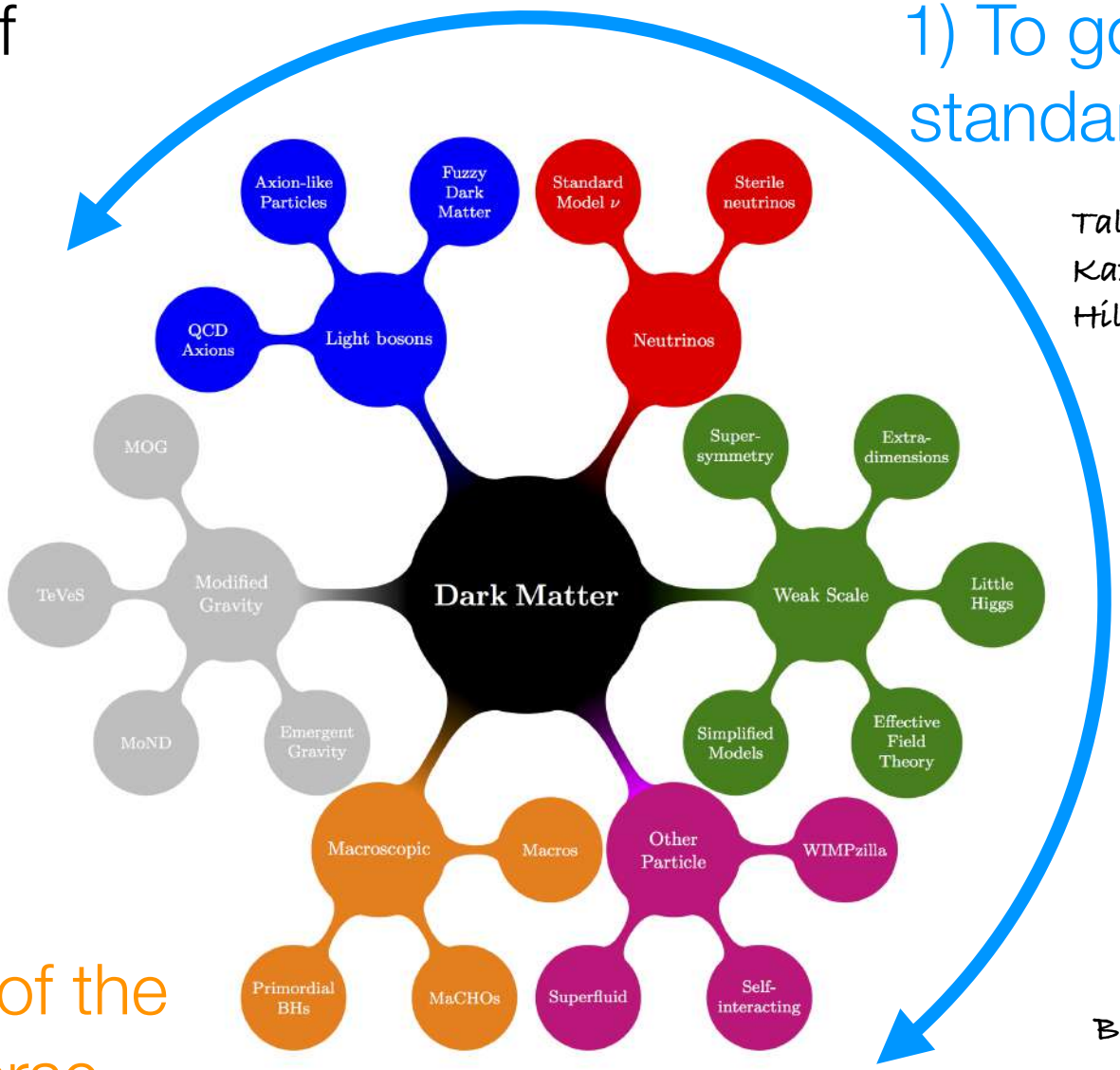
1) To go beyond standard model

Talks by Slatyer, Kazama, Irastorza, Hildebrandt

2) To modify general relativity

tension e.g., w/ Bullet cluster

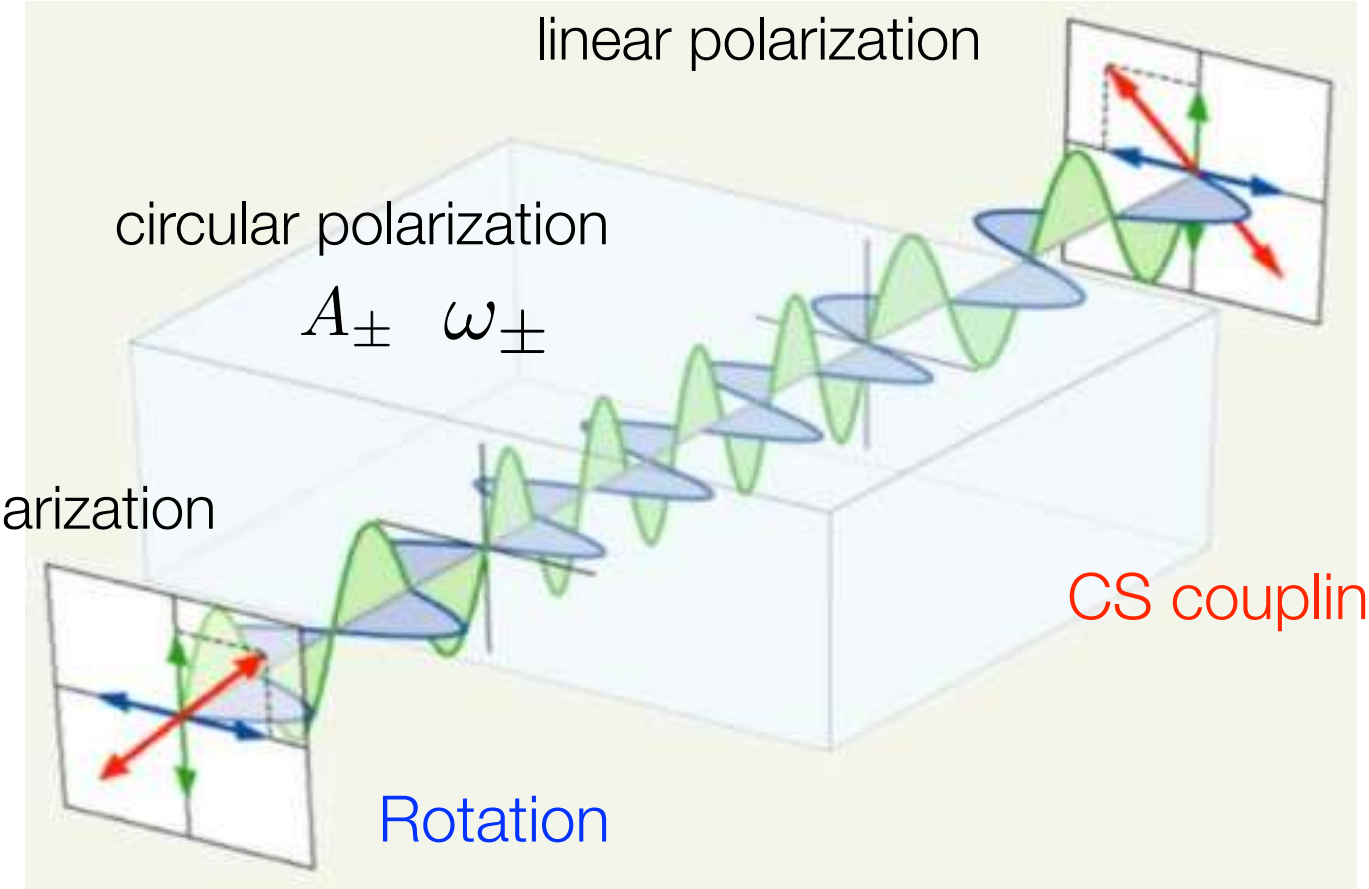
Clowe et al. (06)



3) To modify map of the primordial Universe

Bertone & Tait (18)

Cosmic birefringence as probe of ALP DM



CS coupling $\frac{g_{a\gamma}}{4}\phi F_{\mu\nu}\tilde{F}^{\mu\nu}$

Harari & Sikivie (1992)

$\omega/m \gg 1$

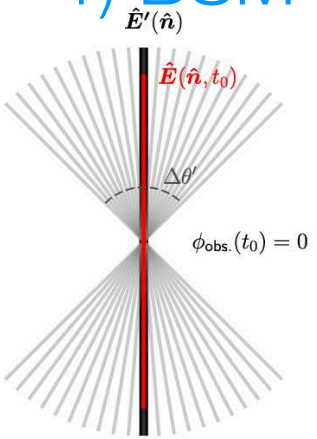
(geometrical optics approx)

$$\Delta\theta_a = \frac{g_{a\gamma}}{2}\left[\phi(t_{\rm obs}, x^i_{\rm obs}) - \phi(t_{\rm em}, x^i_{\rm em})\right]$$

AC effects **source effects**

1) BSM

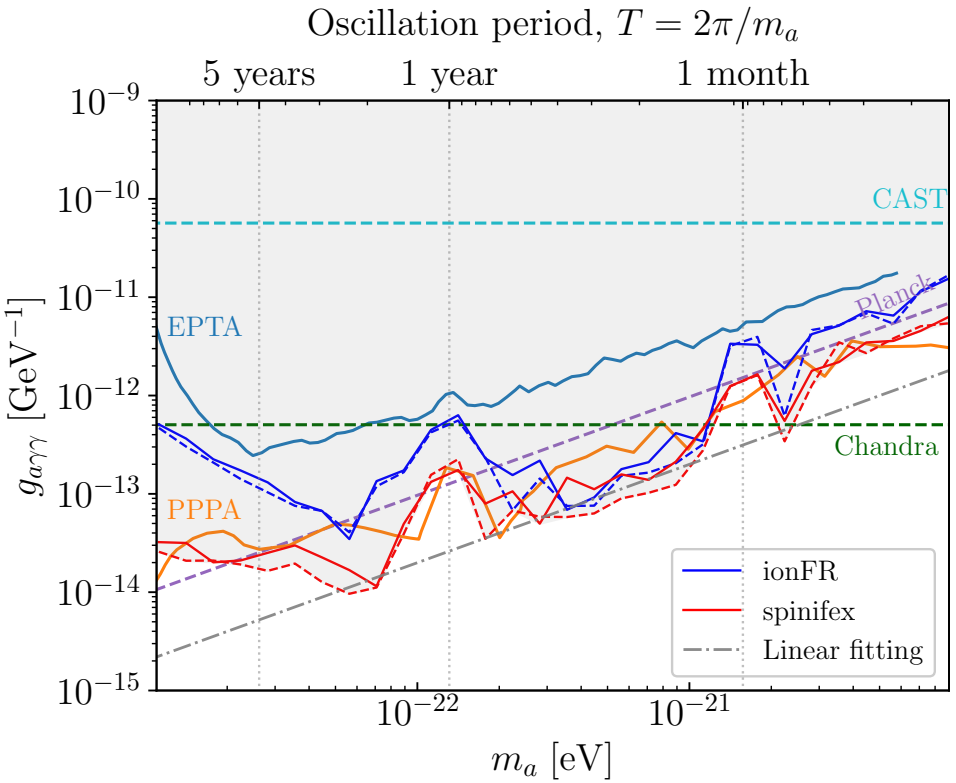
Birefringence as probe of ALP DM



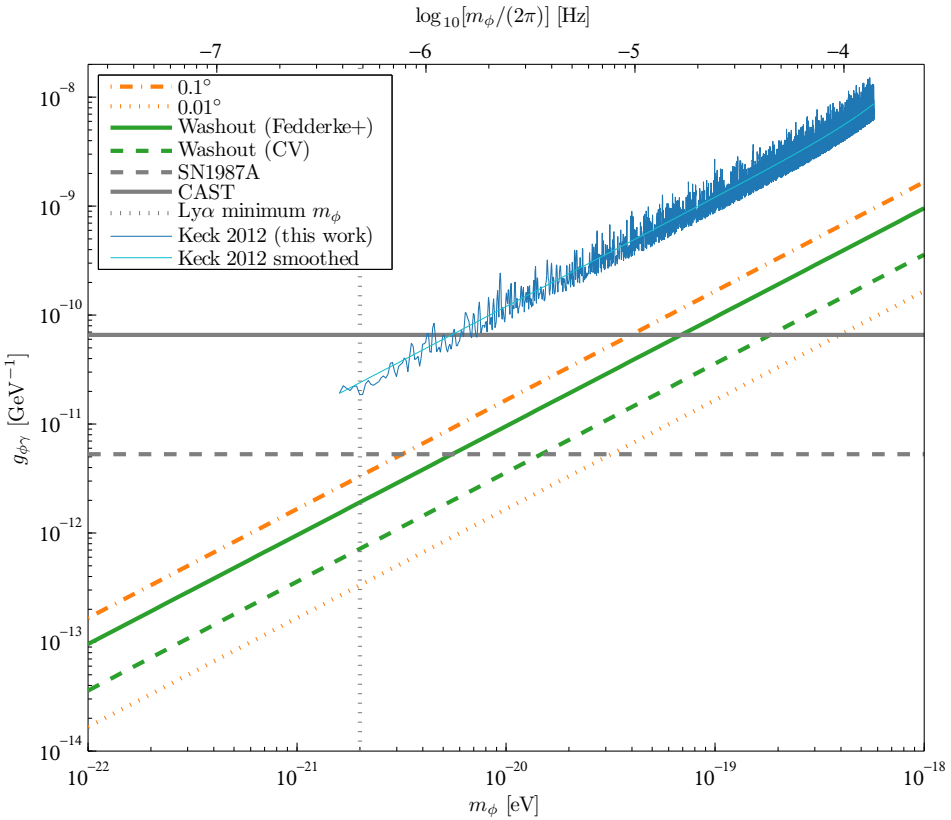
AC effects

Source effects (Wash-out)

Polarized Pulsar Array



CMB



MeerKAT Yuwen et al. (26)

BICEP/Keck collaboration(20)

Mitigation of calibration errors

Credit; Minami and Komatsu



We could only measure the sum $\alpha + \alpha_{\rm mis}$

Use the polarized dust emission within milky way as a calibrator,
since the miscalibration ($\alpha_{\rm mis}$) rotates both CMB and foreground but α only affects CMB.

→ $\alpha = 0.35 \pm 0.14$ deg (68%CL) *Minami & Komatsu (20)* # citation > 500

Planck DR4 + ACT DR6 $\alpha = 0.277 \pm 0.057$ *Eskilt (26)*

For an interpretation of this, see e.g., *Namikawa, Murai, Naokawa (25)* lighter than ALP DM

Axion/ALP and (small-scale) structure formation

Axion dark matter

Tracy Slatyer's talk

- PQ sym broken already during inflation typically $f_{\rm PQ} \geq H_{\rm inf}$

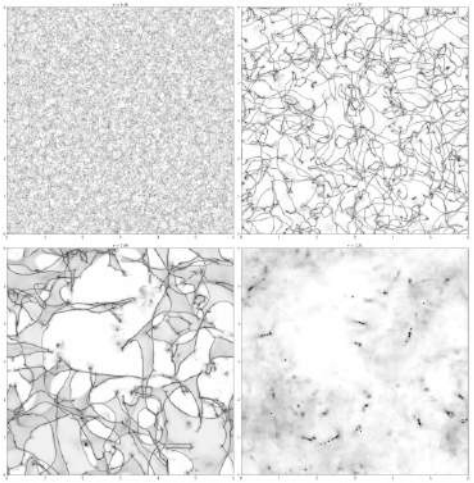
Isocurvature restricts $H_{\rm inf}$ typically $H_{\rm inf} < 10^7 {\rm GeV}$

- PQ sym broken after inflation typically $f_{\rm PQ} < H_{\rm inf}$

Axion mini-cluster formation

strong lensing, pulsar,….

Kolb&Tkachev(95), Fairbairn et al. (17), Dai&Miralda-Escude(19)



Vaquero, Redondo, Stadler (18)

Fuzzy DM (ALP w/$m_a \sim 10^{-22}$eV)

de Broglie wavelength $\lambda_{\rm dB} \equiv \frac{2\pi}{mv} = 0.48\,{\rm kpc}\left(\frac{10^{-22}\,{\rm eV}}{m}\right)\left(\frac{250\,{\rm km\,s^{-1}}}{v}\right)$

e.g., Dalal et al. (2020)

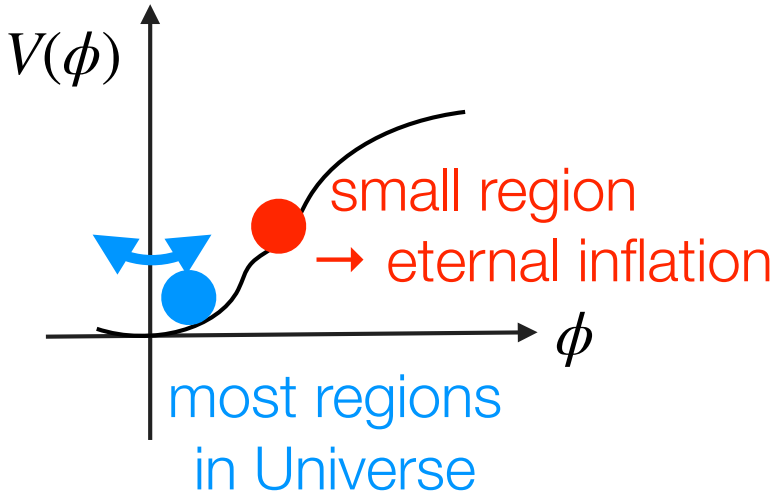
Yet, tension w/Lyman α, dwarf galaxies,… for $\Omega_{\rm FDM}/\Omega_m \sim 1$

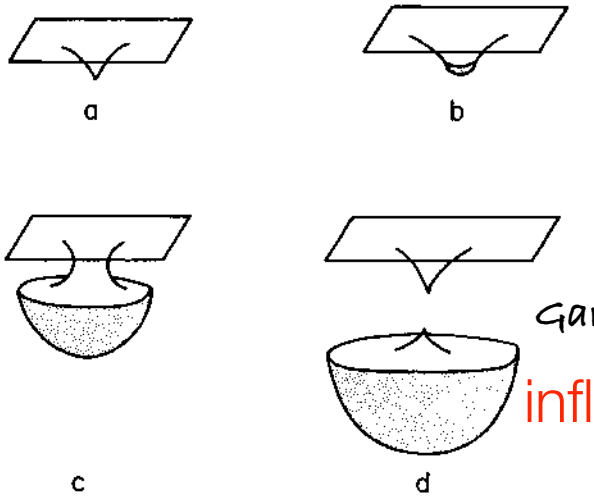
$m_a > 3 \times 10^{-19}{\rm eV}(99\,\%\,{\rm CL})$

Dalal and Kravtsov (2022)

Something more eccentric

one of two origins of PBH Blau, Guendelman, and Guth (1987)

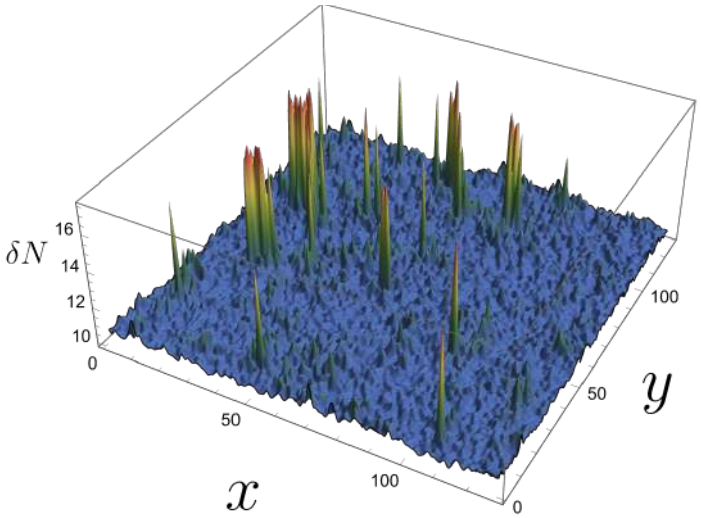




external observer
recognises it as BH

Garriga, Vilenkin, Zhang (16)

inflation
(baby universe)



Numerical simulation can follow the dynamical BH formation.

Saha, Tada, Y.U. (26), Saha, Sasaki, Y.U. (in prep)

simulation during inflation

Caravano et al. (24, 25, 26), Figueroa et al. (25),.....

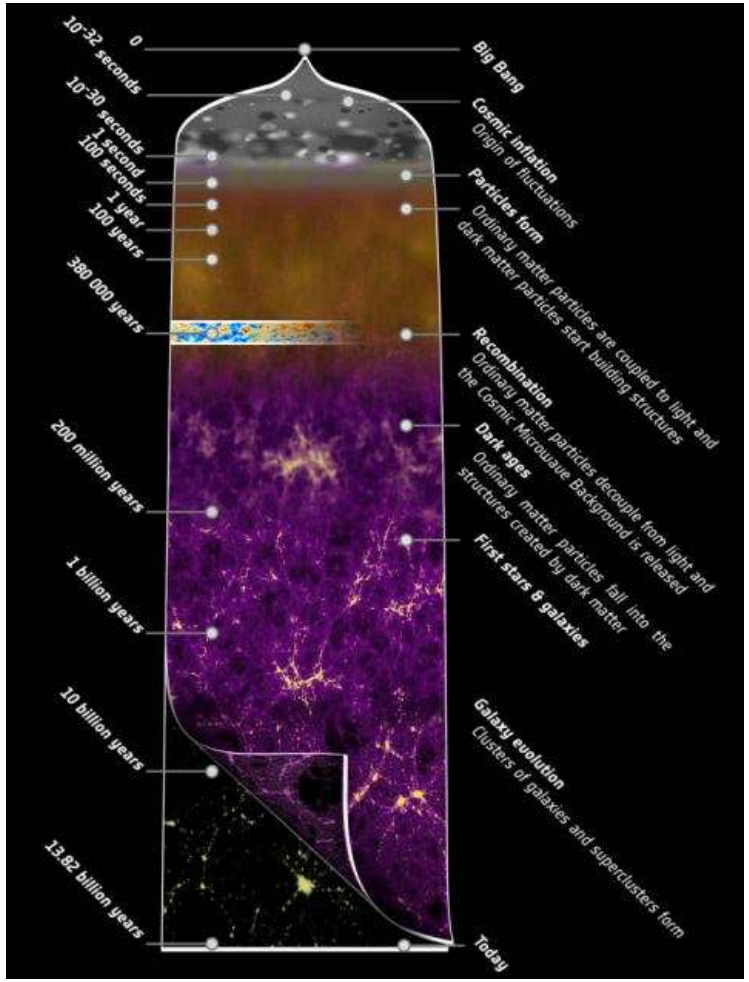
Outline

We know the gross picture of the cosmic history but the microphysics/origins remain unknown.

1) Initial conditions of Big Bang cosmology and inflation

2) Structure formation and dark matter

3) Accelerated expansion and dark energy

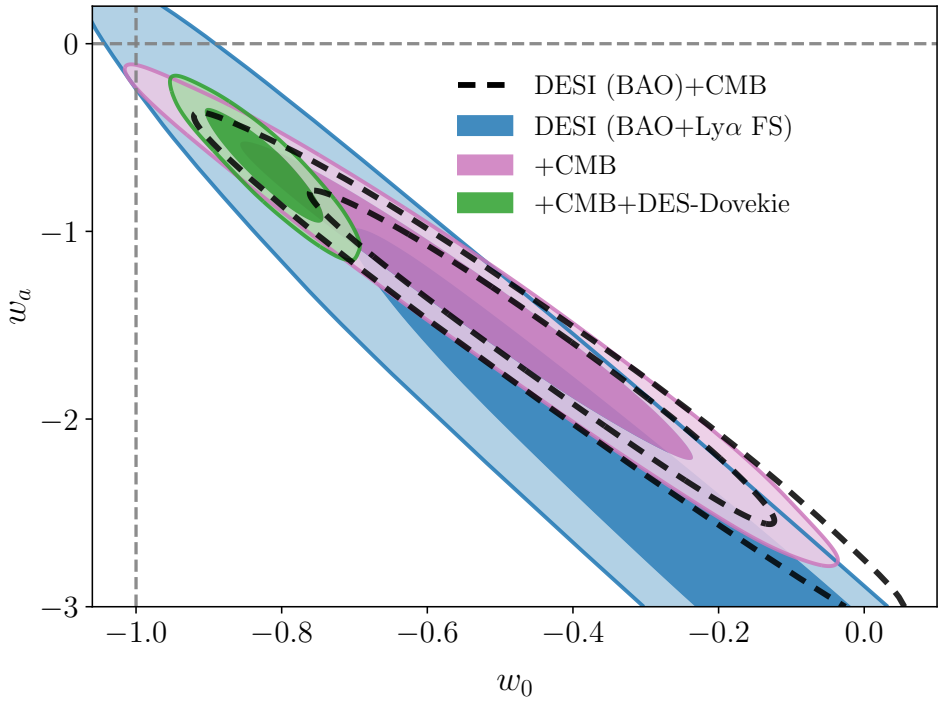


DESI as a trigger of theoretical studies

dark energy spectroscopic instrument (DESI)

DR2 (2026)

citation of DR1(Apr. 2024) > 2,200



Slightly reduced but persistent preference for dynamical DE.

- Beyond CPL : parametrization dep. and reconstruction of DE evolution

$$\omega(a) = \omega_0 + \omega_a(1-a)$$

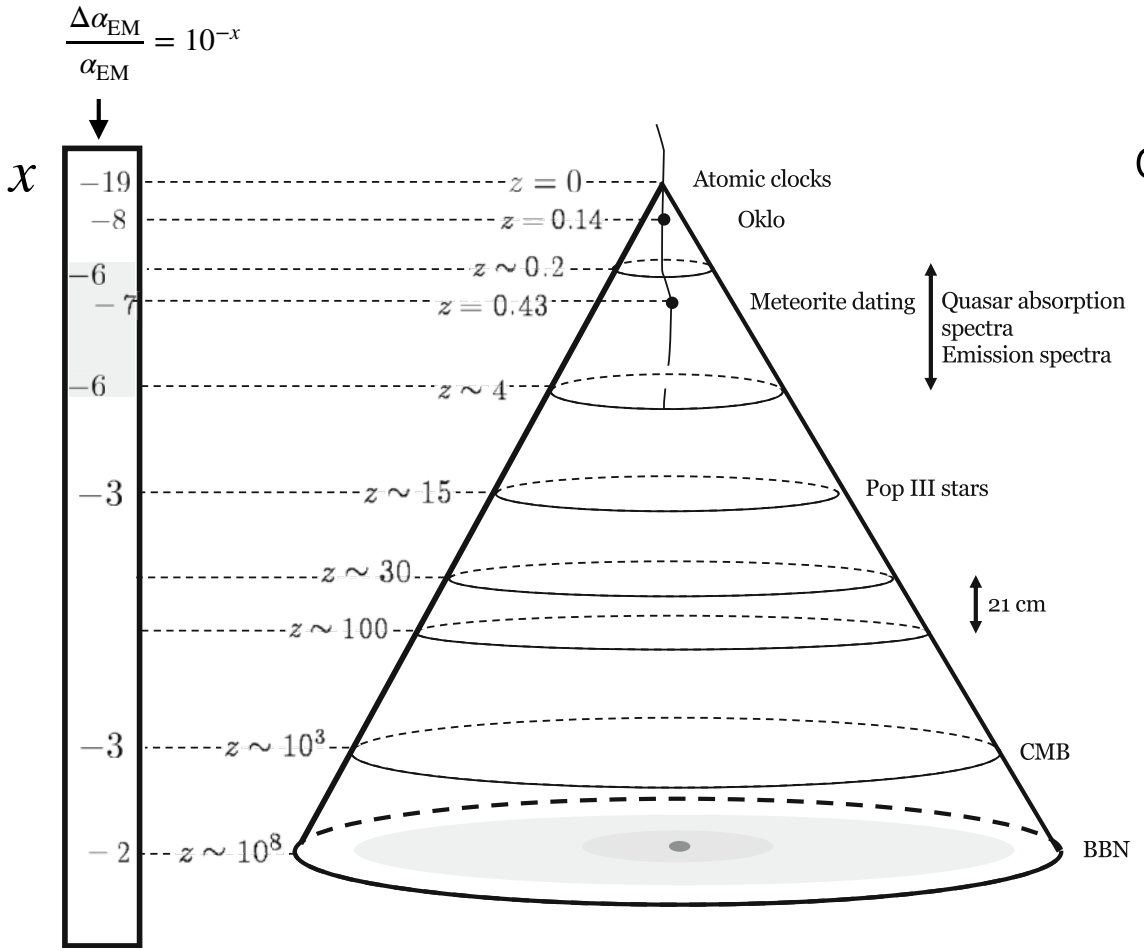
- Theoretical consistency and stability of phantom crossing.

- The fluctuation of dark energy

(if it were to be dynamical)

see Masamune's talk

Constraints on fundamental constants



[Uzan 2410.07281]

- If DESI is true, it might motivate light dilaton phenomenology more seriously.

- If $m_i(\phi) = A(\phi) m_i^{(0)} \qquad (i = e, p, \cdots)$

e.g., C.Burgess (2025)

fifth force problem needs to be addressed together

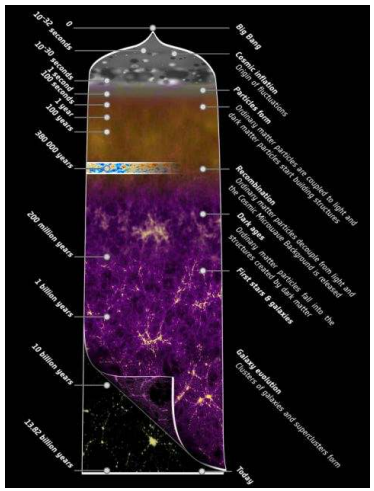
relaxes Hubble tension?

Sekiguchi & Takahashi (2020)

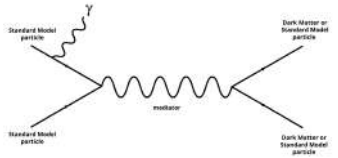
Outlook

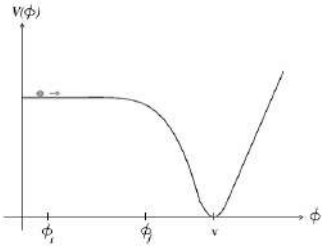
It's an exciting epoch to explore microphysics/origins, going beyond the gross picture of the cosmic history.

CMB, Galaxies, DM halos,…



macro **micro**





dark matter lab searches, CP violation, neutrinos, atomic experiment….

other topics Matter-antimatter asym, reheating, Neutrinos,…

multi-band GW exp.

Marica's talk

Masamune's talk

Progress requires connecting cosmological observations with laboratory tests and theoretical consistency.

Supplement

Distance conjecture

slide from Y. Hamada (KEK)

[Ooguri-Vafa '06]

The Lagrangian of the massless scalar field is

$$\mathscr{L} = \frac{1}{2}\eta^{\mu\nu} g_{IJ}(\partial_\mu \phi^I)(\partial_\nu \phi^J)$$

g_{IJ} is called field space metric. The field space distance is defined from g_{IJ}.

$$(\text{distance from } \phi_0 \text{ to } \phi_1 \text{ with path A}) = \int_{\phi_0}^{\phi_1} ds, \qquad ds^2 = g_{IJ} d\phi^I d\phi^J$$

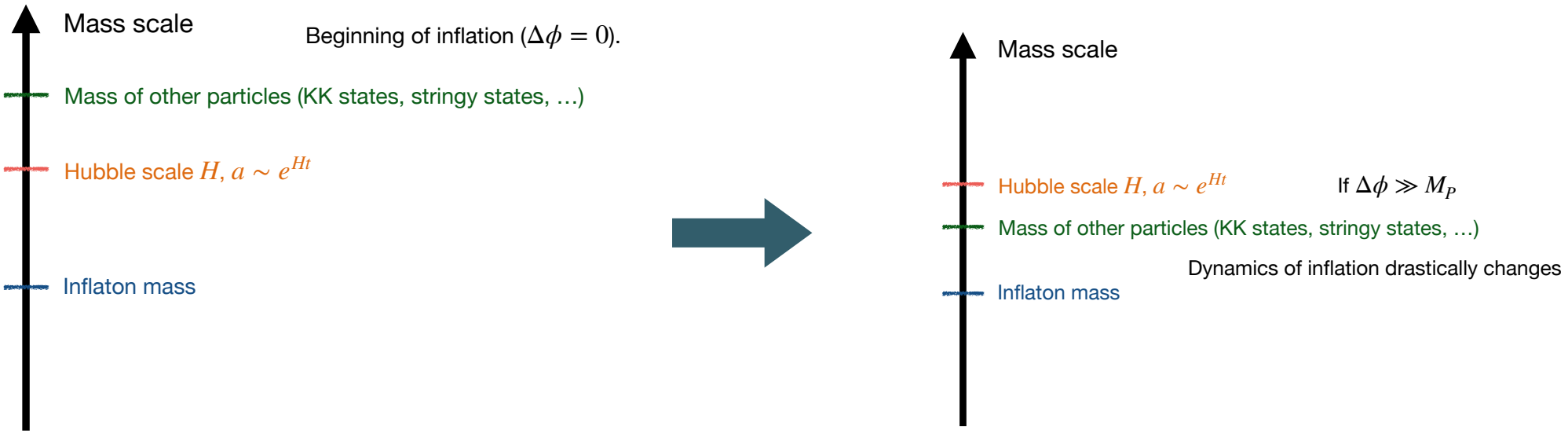
Statement: At large geodesic distance $\Delta\phi \to \infty$ (fixed M_P), the exponentially light tower of state appears.

$$M_{\text{tower}} \sim n M_P e^{-\alpha \Delta\phi}, \qquad \text{for} \quad \Delta\phi \to \infty, \quad n = 1,2,\cdots$$

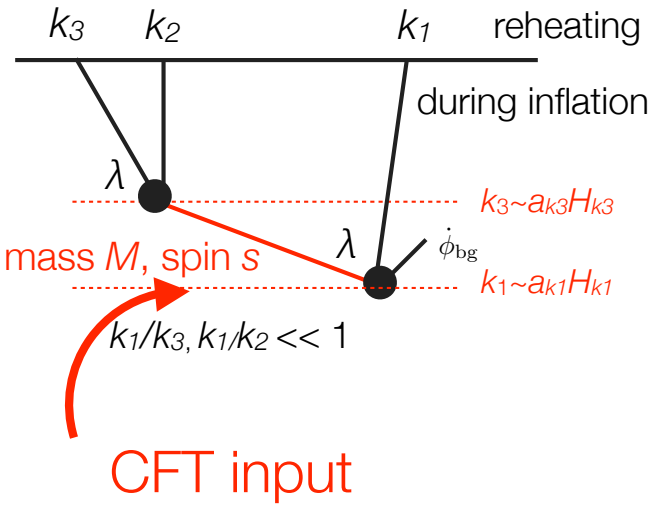
where α is $\mathcal{O}(1)$ positive number.

Typical spectrum during inflation

slide from Y. Hamada (KEK)



Imprint of heavy particles on non-Gaussianity



$$\sim \lambda^2 \dot{\phi}_{\rm bg} e^{-M/T_{\rm H}} \left(\frac{k_1}{k_3}\right)^{\Delta} (\hat{\mathbf{k}}_1 \cdot \hat{\mathbf{k}}_3)^s \mathcal{P}(k_1)\mathcal{P}(k_3)$$

Arkani-Hamed & Maldacena (15)

mass (oscillation due to interference)

spin

$\mathcal{P}(k)$:power spectrum

1) Boltzmann suppression

Higuchi bound $M^2 > s(s-1)\, H^2$

dS — Bordin et al. (18)

global rotation — Kehagias & Riotto (17)

2) Dilution of massive fields

3) Weak coupling

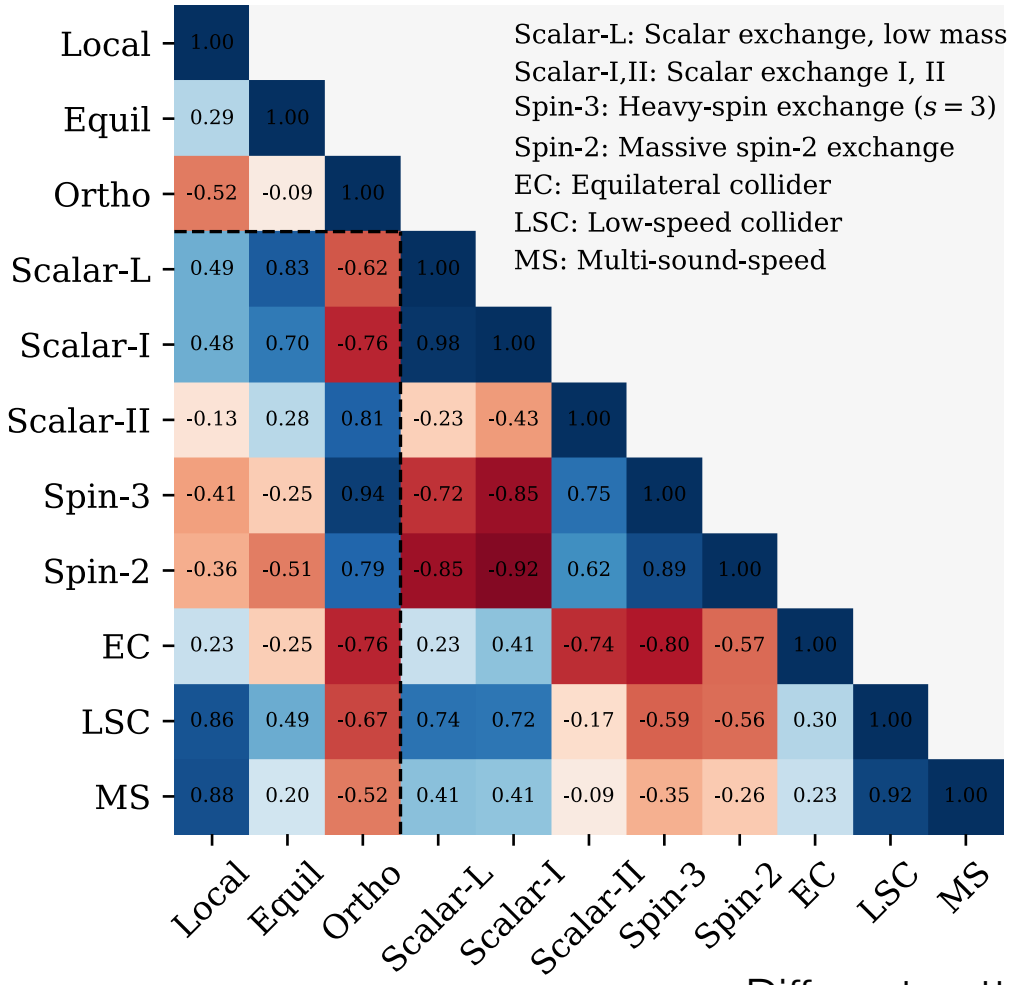
Large coupling tends to make 1) more severe.

Wang & Xianyu (19, 20)

Difficulty

Sohn et al. (24)

strong correlation (+1) or anti-correlation (-1)



Different patters of PNG are correlated.

Models

Nerval, Hlozek, Jense, Bond (2606.28310)

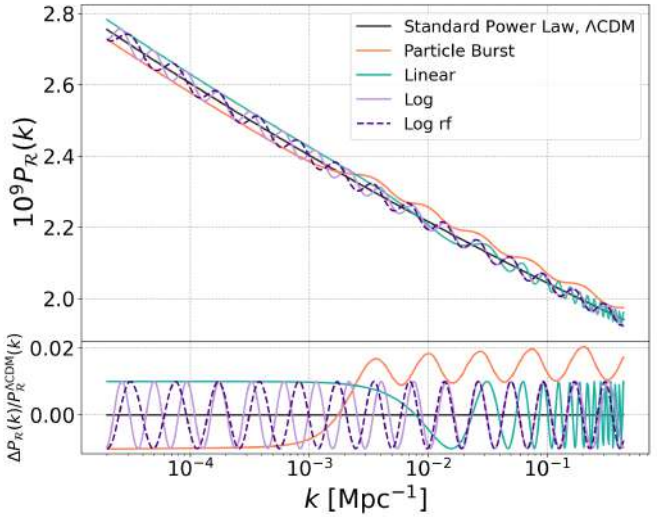
1) General oscillation

$$P_{\mathcal{R}}(k) = A_s \left(\frac{k}{k_*}\right)^{n_s-1} \left[1 + \delta P^X\right]$$

$$\delta P^X = A_X \cos(\omega_X \Xi_X + 2\pi\phi_X)$$

with $\Xi_X = \{k/k_*,\ \ln(k/k_*),\ \ln(k/k_*)(1+\alpha_{rf}\ln(k/k_*))\}$

$X = \{\text{lin},\ \text{log},\ \text{log rf}\}$



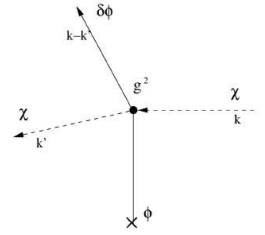
including Axion monodromy inflation → X=log rf Silverstein & Westphal (08)

$$V = \mu_a^3 \phi_a + \Lambda^4 \cos(\phi_a/2\pi f_a)$$

2) Burst particle production

$$\mathcal{L}_{\text{int}} = -\frac{g^2}{2}(\phi-\phi_i)^2\chi^2 - g^2(\phi-\phi_i)\delta\phi\chi^2 - \frac{g^2}{2}\delta\phi^2\chi^2$$

$$P_{\mathcal{R}}(k) = A_s\left(\frac{k}{k_*}\right)^{n_s-1} + A_I\sum_i\left(\frac{f_1(x_i)}{f_1^{\max}}\right) + A_{II}\sum_i\left(\frac{f2(x_i)}{f_2^{\max}}\right)$$



Bremss

Barnaby (10), Pearce t al. (17)

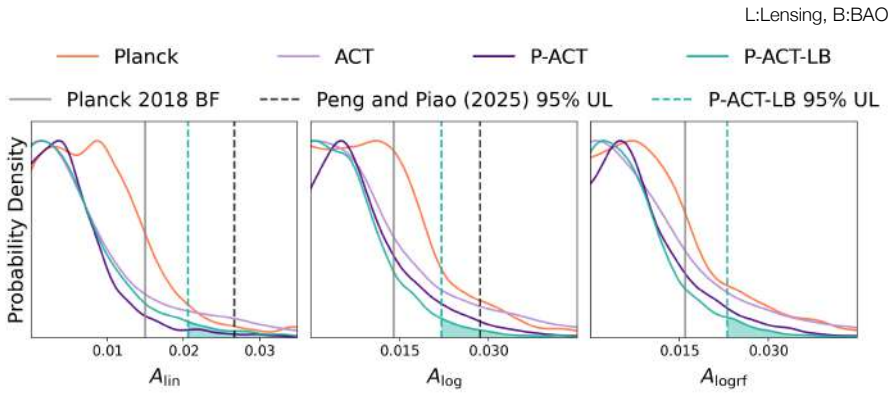
$$x_i \equiv \frac{k}{k_i} \qquad f_1(x_i) \equiv \frac{\left(\sin(x_i) - \text{SinIntegral}(x_i)\right)^2}{x_i^3} \qquad f_2(x_i) \equiv \frac{-2x_i\cos(2x_i) + (1-x_i^2)\sin(2x_i)}{x_i^3}$$

Results

Nerval, Hlozek, Jense, Bond (2606.28310)

1) General oscillation

posterior



Parameter	*Planck*	ACT	P-ACT	P-ACT-LB
$A_{\rm lin}$	< 0.023	< 0.033	< 0.017	< 0.021
$A_{\log}$	< 0.032	< 0.040	< 0.027	< 0.022
$A_{\log\ \rm rf}$	< 0.034	< 0.040	< 0.027	< 0.023

~ 2% bound

	Linear				Log				Log rf			
Parameter	*Planck*	ACT	P-ACT	P-ACT-LB	*Planck*	ACT	P-ACT	P-ACT-LB	*Planck*	ACT	P-ACT	P-ACT-LB
$\log(10^{10}A_{\rm s})$	3.06	3.06	3.05	3.06	3.05	3.05	3.06	3.07	3.05	3.06	3.05	3.06
$n_{\rm s}$	0.965	0.965	0.970	0.975	0.964	0.968	0.971	0.977	0.964	0.968	0.971	0.976
$10^3 A_X$	11.7	9.57	7.91	7.93	8.99	13.7	5.55	8.18	10.7	11.9	9.03	6.96
$\log_{10}(\omega_X)$	1.06	0.972	1.08	1.08	0.994	1.25	1.05	1.06	1.01	1.29	1.05	1.05
ϕ_X	0.447	0.394	0.439	0.510	0.436	0.505	0.681	0.643	0.486	0.459	0.577	0.540
$\alpha_{\rm rf}$	–	–	–	–	–	–	–	–	0.0278	-0.0733	0.0274	0.0506
$\Delta\chi^2$	−8.93	−3.55	−4.68	-5.53	−6.49	−5.26	−6.15	-7.18	−4.98	−6.83	−7.69	-8.70
$\ln B$	−2.60	−2.94	−2.97	−3.84	−2.71	−2.91	−2.81	−3.49	−2.73	−2.95	−2.88	−3.58

Table 3: MAP values for the general oscillation models as well as $\Delta\chi^2$ and $\ln B$ relative to ΛCDM. Negative $\Delta\chi^2$ indicates an improved fit and negative $\ln B$ indicates a preference for ΛCDM. The $\Delta\chi^2$ values are computed using the MAP values, whereas the $\ln B$ values are computed using the evidence value from `pocoMC`.

Marginal improvements in fits yet, but Baysian evidence showed a moderate preference for ΛCDM.

Results

Nerval, Hlozek, Jense, Bond (2606.28310)

2) Burst particle production

posterior

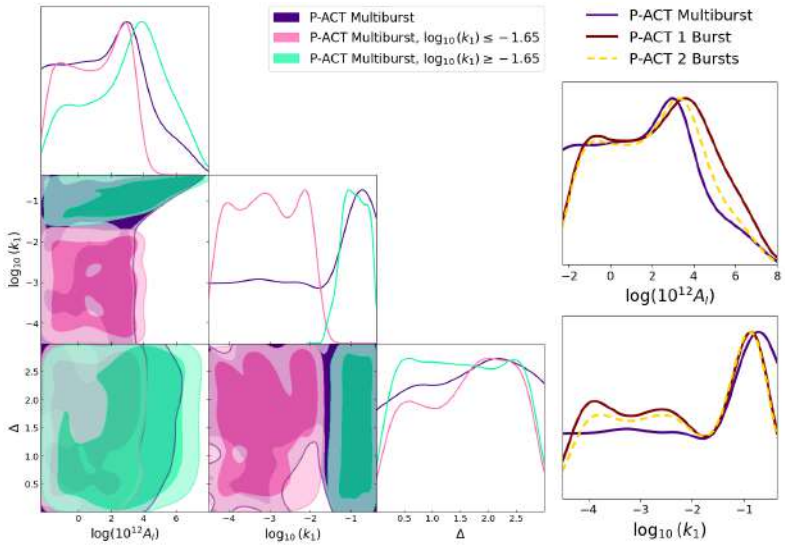


Figure 14: Showing the changes in parameter constraints for the different k-range priors and the number of bursts. *Left:* 1D and 2D posterior distributions using P-ACT for the multiburst particle model for the full k-range (indigo), $\log_{10}(k_1) \leq -1.65$ (light green) and $\log_{10}(k_1) \geq -1.65$ (pink). *Right:* 1D posterior distributions using P-ACT for the particle model for 1 burst (maroon), 2 bursts (yellow), and 10 bursts (indigo) for the amplitude and initial burst position.

Parameter	Multiburst		1 Burst	2 Bursts	$\log_{10}(k_I) \geq -1.65$	$\log_{10}(k_I) \leq -1.65$
	P-ACT	P-ACT-LB				
$\log(10^{10}A_s)$	3.05	3.05	3.05	3.05	3.04	3.03
n_s	0.971	0.973	0.970	0.974	0.967	0.970
$\log(10^{12}A_I)$	2.10	1.56	1.80	2.70	3.04	3.80
$\log_{10}(k_1)$	-1.08	-1.29	-3.00	-2.37	-1.23	-2.77
Δ	0.890	0.785	–	0.737	0.629	0.876
$\Delta\chi^2$	−1.35	−0.12	−0.50	−2.90	−3.55	−1.40
$\ln B$	−0.08	−0.23	0.03	−0.05	0.30	−0.40

Table 4: Combined MAP values for the particle burst model from the `Cobaya` minimizer, including the P-ACT-LB dataset. $\Delta\chi^2$ and $\ln B$ are relative to ΛCDM. The $\Delta\chi^2$ values are computed using the MAP values, whereas the $\ln B$ values are computed using the evidence value from `pocoMC`. Negative $\Delta\chi^2$ indicates an improved fit and negative $\ln B$ indicates a preference for ΛCDM.

Marginal improvements in fits yet, but Baysian evidence is inconclusive.

Non-linear matter PS

Nerval, Hlozek, Jense, Bond (2606.28310)

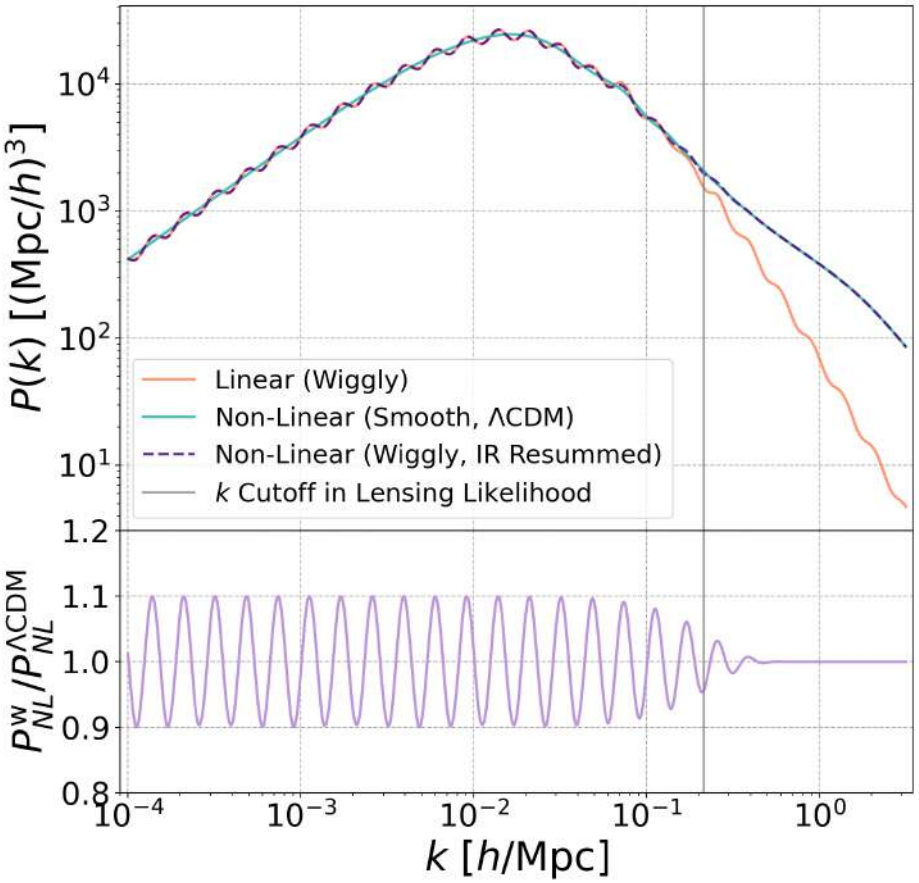
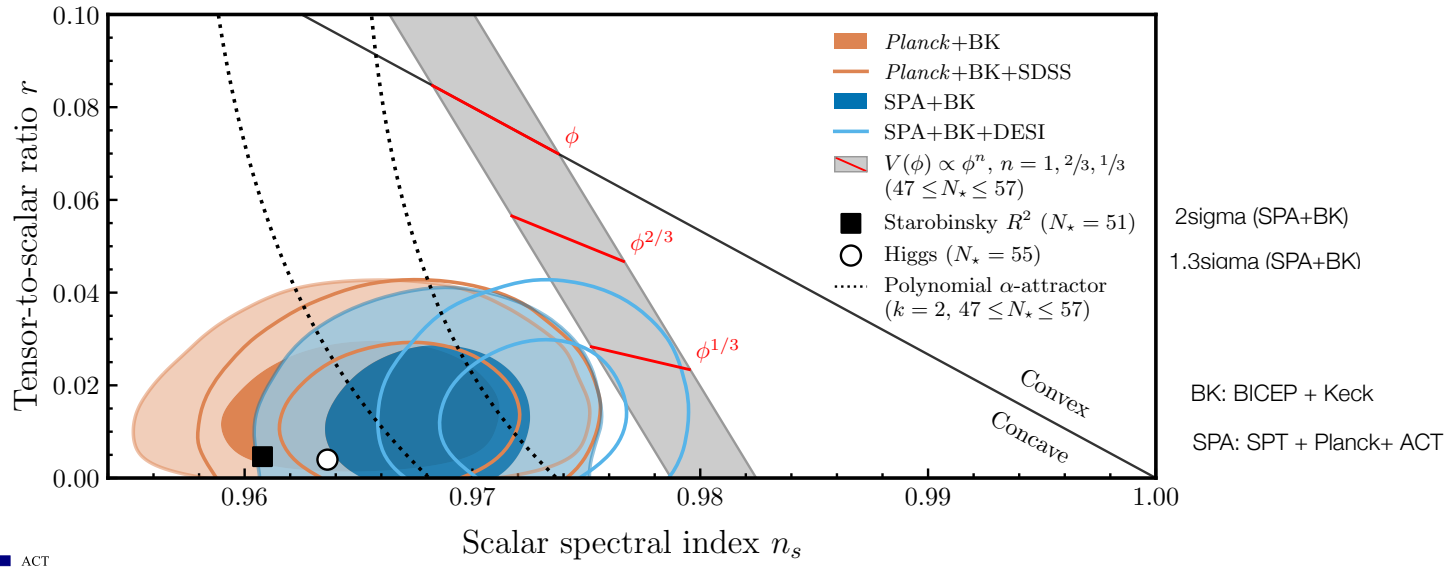


Figure 18: Comparison of the linear and non-linear matter power spectra computed using the accuracy settings for `CAMB` shown described in Appendix A of C25. We use the IR resummation corrections to the non-linear power spectrum outlined in Eq. C.1 and Ref. [44]. The bottom panel displays the ratio of oscillatory and baseline ΛCDM power spectra.

(n_s, r) plot

Balkenhol et al. (26)
2512.10613

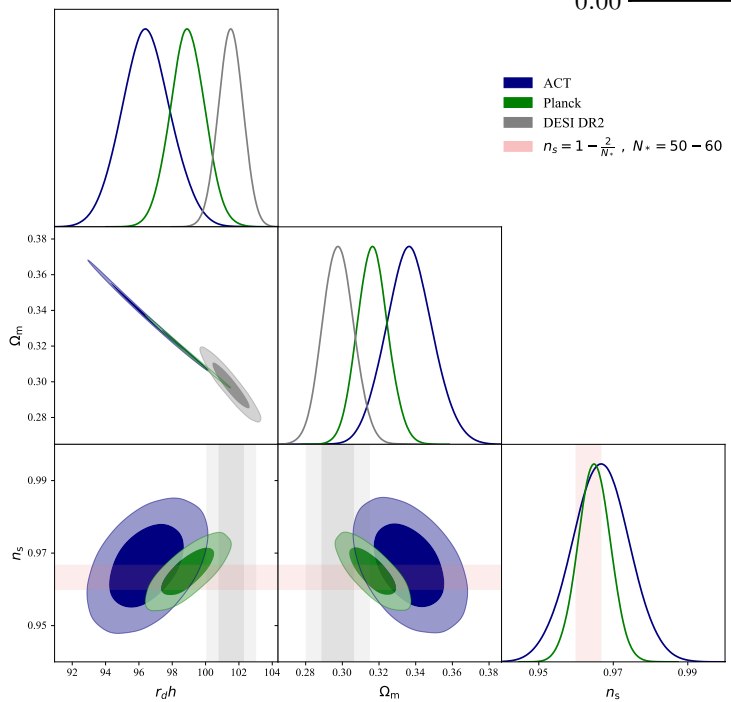


2sigma (SPA+BK)

1.3sigma (SPA+BK)

BK: BICEP + Keck

SPA: SPT + Planck+ ACT



- $r < 0.034,\ n_s = 0.9682 \pm 0.0032$

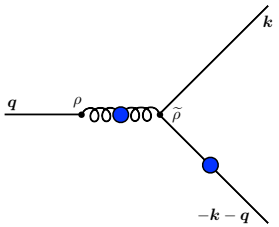
(SPA+ BK, 95%)

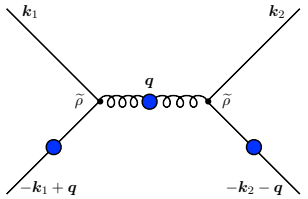
Ferreira et al. (25) 2507.12459

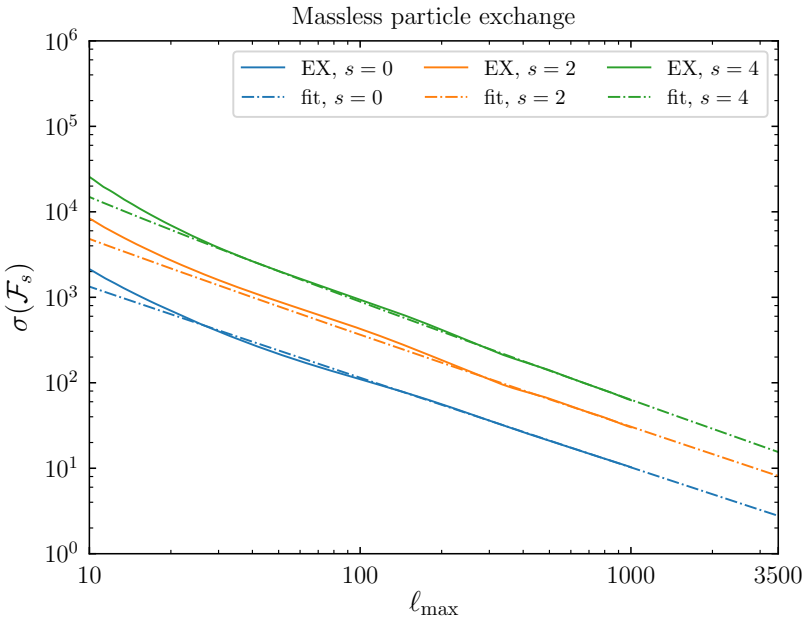
FIG. 1. Comparison of CMB data sets: Constraints from ACT and *Planck*. Overlaid are constraints on BAO parameters from DESI DR2 (grey bands). Pink shaded bands show the spectral index $n_s = 1 - 2/N_*$, as predicted by the Starobinsky, Higgs, and exponential α-attractor models, for $N_* = 50 - 60$.

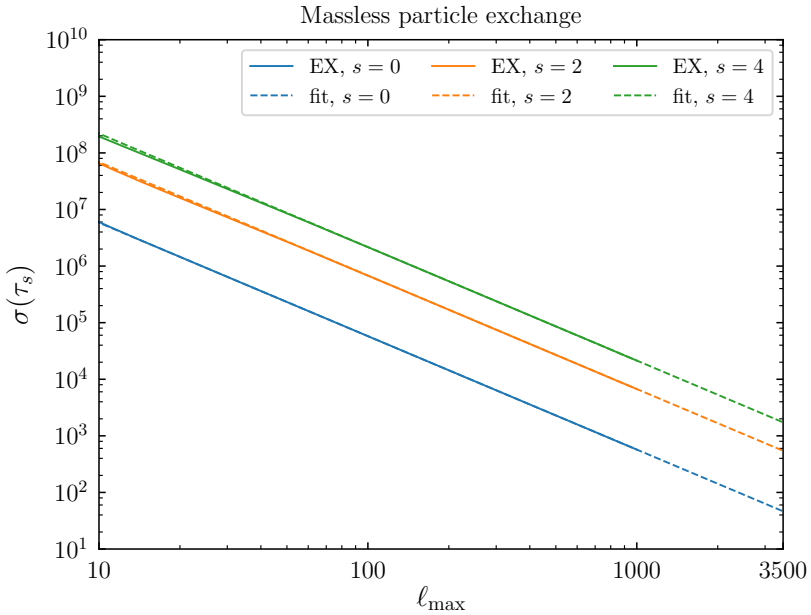
CMB constraints from PLANCK (Massless)

Bordin & Cabasse(18)







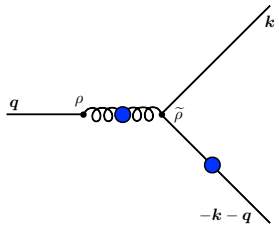


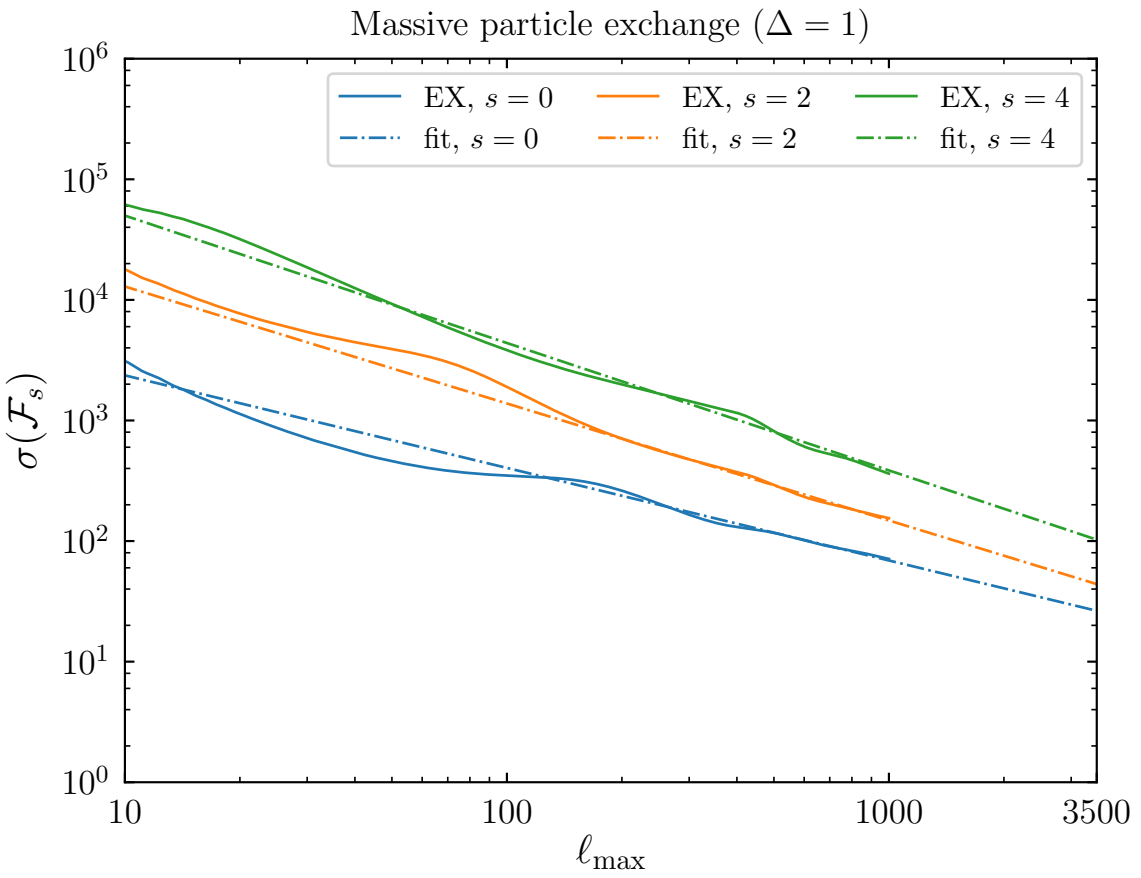
Up to which (small) angle?

s=2, 4 are not compatible with Higuchi bound (dS).

CMB constraints from PLANCK (Massive)

Bordin & Cabasse(18)



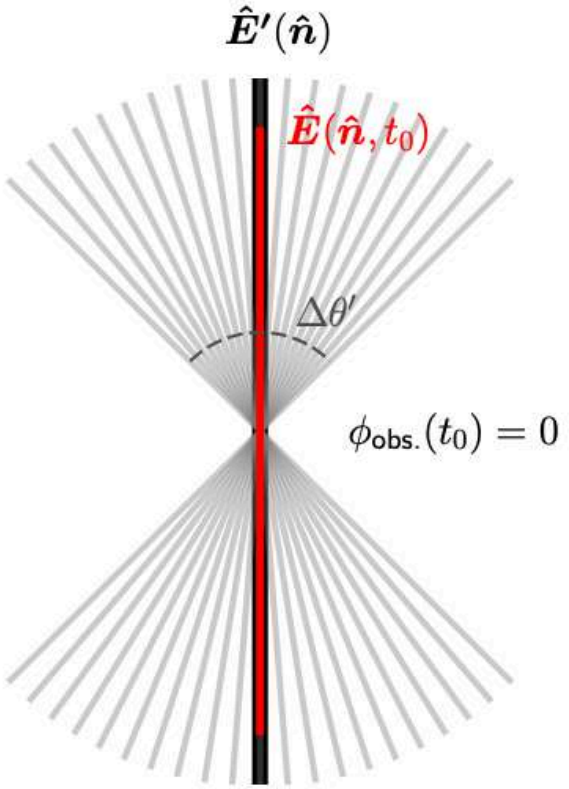


Marginally satisfies Higuchi bound (dS).

Birefringence on CMB: Washout effect

Fedderke et al. (19)

Washout (@LSS) * not actual time variation



visibility fn. has thickness of $\Delta z \sim 200$

Last scattering occurs in $\sim 10^5$ yrs

$>> T_\phi \sim 0.1$ yrs (10^{-21}eV/m)

Net amplitude at LSS is smeared

Birefringence on CMB

Fedderke et al. (19)

Inhomogeneous patches
(k/a >> m)

$$\Delta\theta = \frac{g_{a\gamma}}{2}\left[\phi(t_{\rm obs}, x^i_{\rm obs}) - \phi(t_{\rm em}, x^i_{\rm em})\right]$$

Last scattering occurs in ~10^5 yrs

>> T_ϕ ~ 0.1 yrs (10^{-21}eV/m)

For |f(t)| << 1 with $f(t) \equiv g_{\phi\gamma}\phi_0 \cos(mt + \alpha)$

$$\begin{pmatrix} Q(\hat{\mathbf{n}}, t) \\ U(\hat{\mathbf{n}}, t) \end{pmatrix} = \begin{pmatrix} 1 & -f(t) \\ f(t) & 1 \end{pmatrix} \begin{pmatrix} \langle Q(\hat{\mathbf{n}}) \rangle \\ \langle U(\hat{\mathbf{n}}) \rangle \end{pmatrix}$$

AC effect — Washout effect

Oscillation at observer — Smearing

CMB birefringence

$$C_\ell = \frac{\sin 4\beta}{2}(C_\ell^{\mathrm{EE,lss}} - C_\ell^{\mathrm{BB,lss}})$$

$$\mathcal{L} \supset -\frac{1}{4} g\phi F_{\mu\nu}\tilde{F}^{\mu\nu}$$

$$\beta'(\eta) = \frac{1}{2} g\phi'(\eta)$$

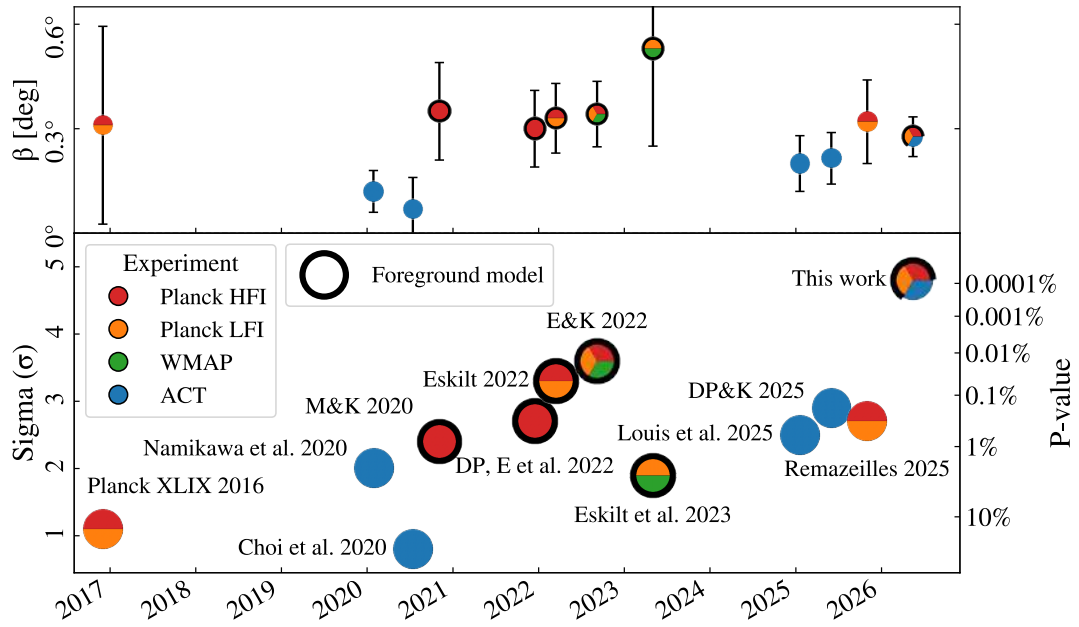


FIG. 4: Timeline of cosmic birefringence measurements in *WMAP*, ACT and *Planck*. The upper panel shows β measurements, and the lower shows the significances. The black rings indicate if a foreground EB model was used.

If this signal were to be real,……

the preferred mass range of ALP is….

Namikawa, Murai, Naokawa (25)

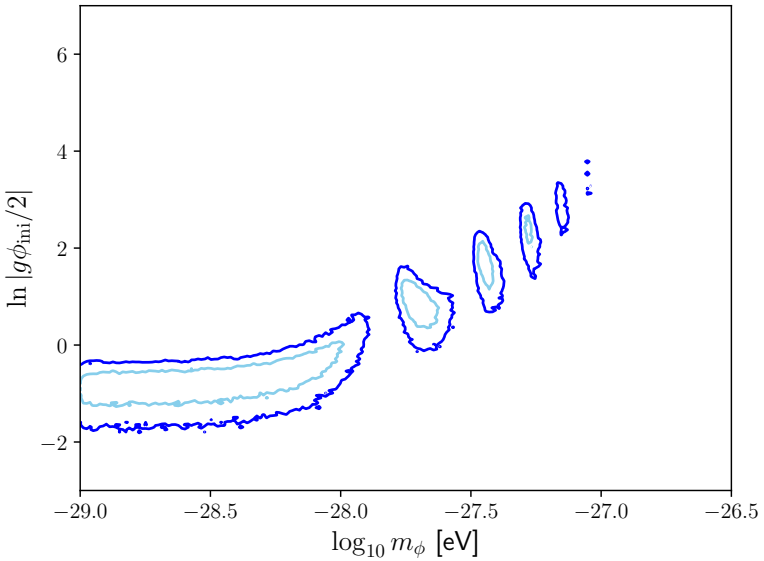


FIG. 2. Same as Fig. 1, but shown in the $\log_{10} m_\phi$[eV]–$\ln|g\phi_{\rm ini}/2|$ plane, where $g\phi_{\rm ini}/2$ is expressed in degrees. The two-dimensional posterior is visualized with $1\,\sigma$ (cyan) and $2\,\sigma$ (blue) contours.

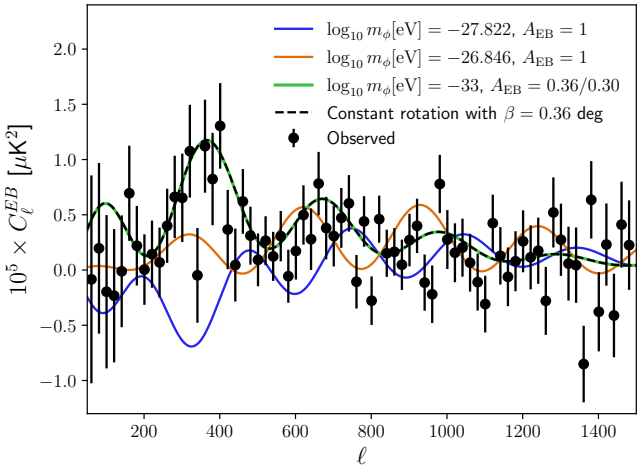


FIG. 3. Comparison of theoretical EB power spectra for different ALP masses and amplitudes: $\mu_\phi = -27.822$, $A_{\rm EB} = 1$ (blue solid), $\mu_\phi = -26.846$, $A_{\rm EB} = 1$ (orange solid), and $\mu_\phi = -33$, $A_{\rm EB} = 0.36/0.3$ (green solid). For reference, the spectrum from a constant rotation angle $\beta = 0.36$ deg is shown as a black dashed line. The black points represent the stacked, foreground-subtracted EB power spectrum derived from the data using the best-fit foreground model.

* In this regime, the washout is not significantly important.

Bias of galaxies, halos etc…

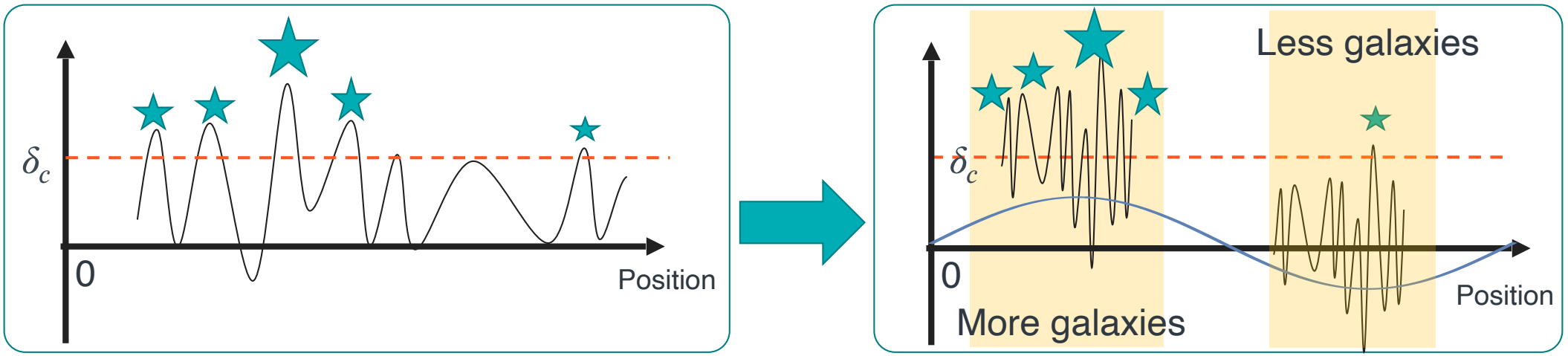
Dark matter

Energy density $\delta_{\rm m} \equiv \dfrac{\rho_{\rm m} - \bar{\rho}_{\rm m}}{\bar{\rho}_{\rm m}}$

Astrophysical objects

(Galaxy)number density $\delta_{\rm n} \equiv \dfrac{n - \bar{n}}{\bar{n}}$

Formation of astrophysical objects are affected by the potential well of gravity.



Decomposing long and short modes

Blue: DM energy density

galaxy, halo etc… number counts are not independent of DM energy density

e.g., For initial Gaussian case $\delta_{\rm n}(\boldsymbol{x}) = b_\delta^{(0)} \delta_{\rm L}(\boldsymbol{x})$

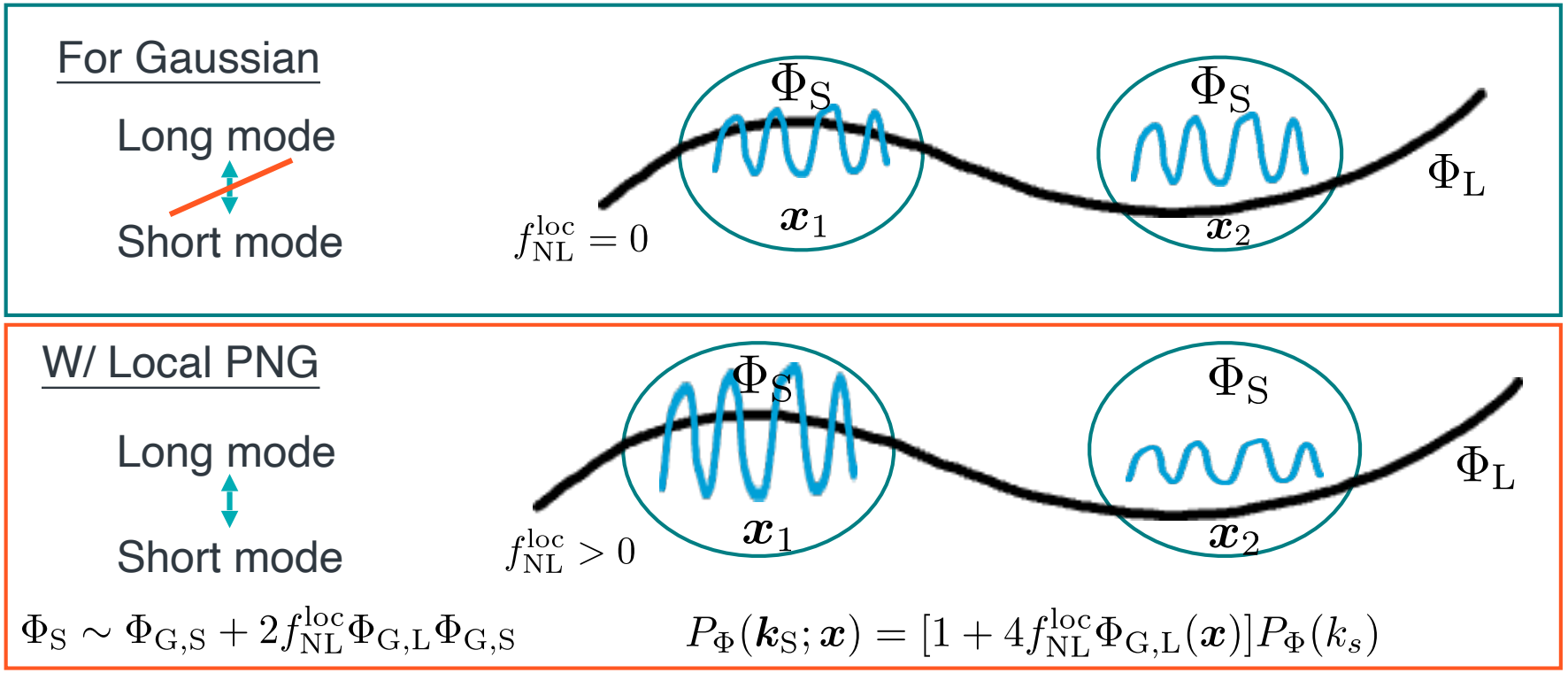
$b_\delta^{(0)}$: bias parameter

W/ (local) PNG

In the presence of local-type non-Gaussianity

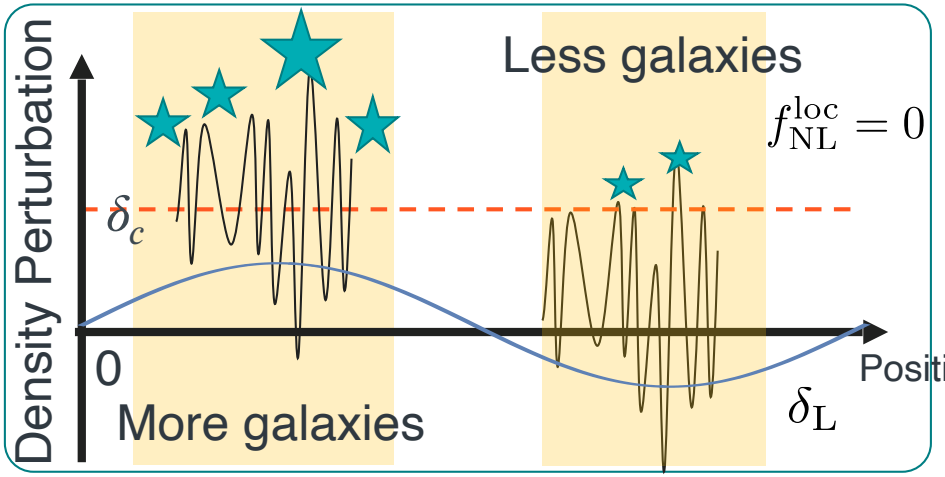
eg. Squeezed bispectrum

(Correlation between short and long modes)



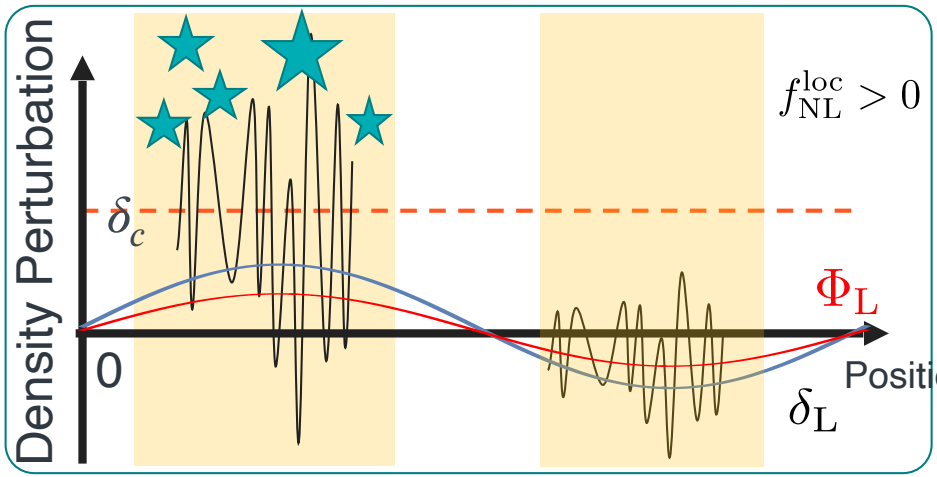
Scale dependent bias

Gaussian at the onset of structure formation
(Initial)



W/ (Local) PNG

Further less galaxies



Further more galaxies

$$\delta_{\rm n}(\boldsymbol{x}) = b_\delta^{(0)}\delta_{\rm L}(\boldsymbol{x}) + b_{\rm NG}^{(0)}\left[4 f_{\rm NL}^{\rm loc}\Phi_{\rm L}(\boldsymbol{x})\right]$$

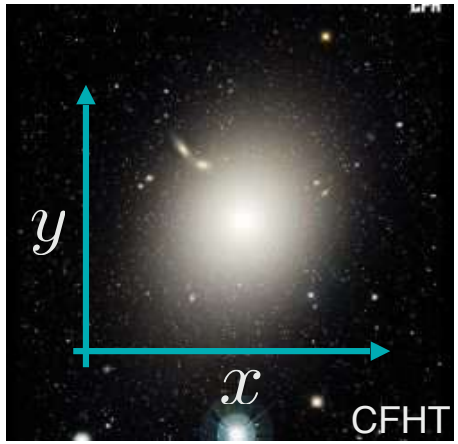
Size of local PNG

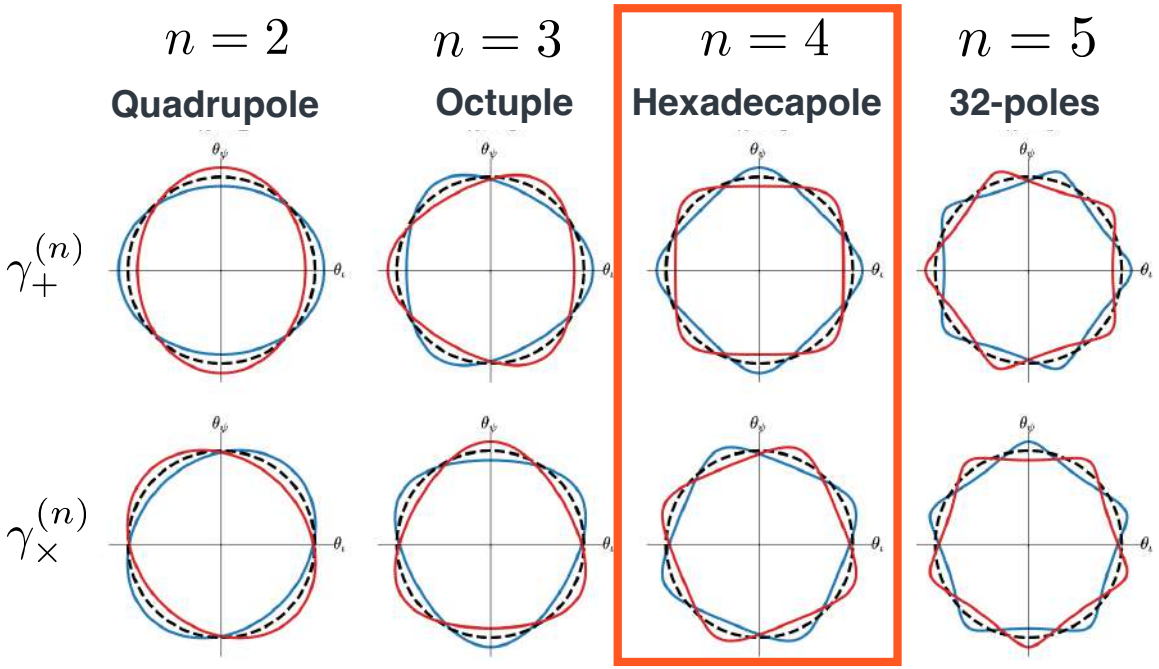
Detailed shapes of galaxies

Mathematically, we can characterize the galaxy shapes in more detail.

Galaxy shapes (n-th moment)

$$\gamma_{i_1 i_2 \cdots i_n}(\boldsymbol{\theta}) \propto \int d^2\theta I(\boldsymbol{\theta}) \theta_{i_1} \theta_{i_2} \cdots \theta_{i_n}$$
$$\theta_{i_n} = (x, y)$$

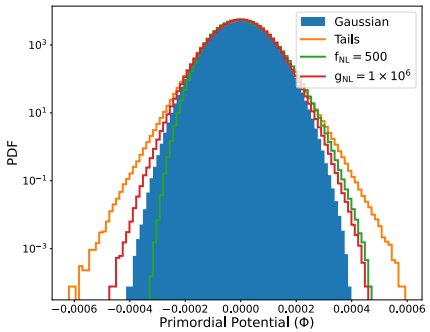




Current observations target this.

Decomposition

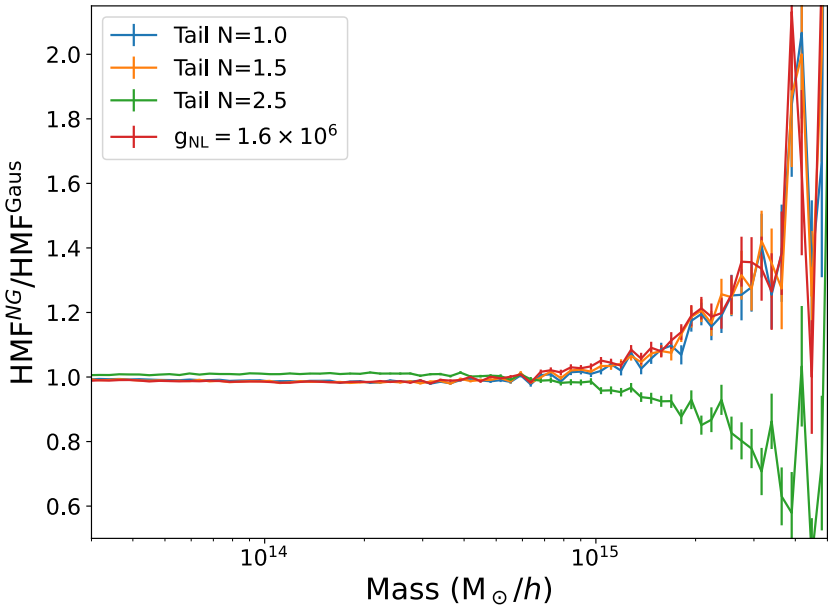
Impact of non-Gaussian tail on halo mass function



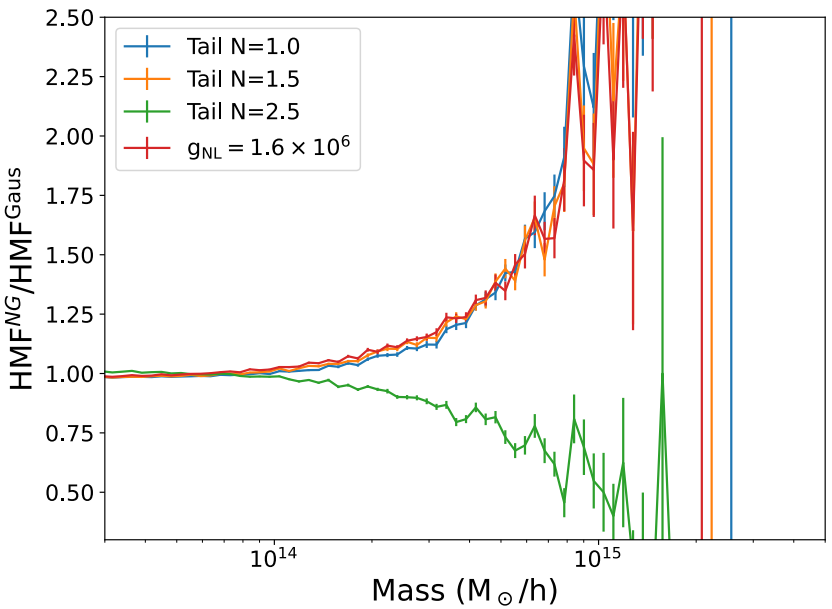
PDF ~ (A exp{−CΦ^N } if |Φ| > ασ,
B exp{− Φ^2/2σ^2 } if |Φ| ≤ ασ.

… and scale dependent bias, cold/hot spots in CMB, and so on

Coulton, Philcox, Villaescus-Navarro (24)



(a) $z = 0.0$



(b) $z = 1.0$

… yet $g_{NL} = -5.8 \pm 6.5 \times 10^4$ (PLANCK18), so excluded 20σ

Theoretical implications of phantom crossing

$$\mathcal{L}_\phi = P(\phi, X) \qquad X \equiv -\frac{1}{2} g^{\mu\nu} \partial_\mu \phi \, \partial_\nu \phi$$

Vikman (04)

Background

$\rho_\phi + p_\phi = 2XP_{,X}$ phantom crossing from $\omega < -1$ to $\omega \geq -1$

→ from $P_{,X} < 0$ to $P_{,X} \geq 0$

Linear Perturbation

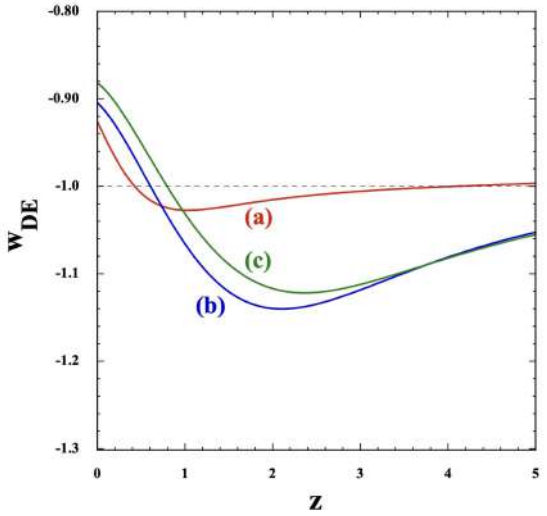
$$S^{(2)} = \frac{1}{2} \int dt \, d^3x \, a^3 \left[K \delta\dot{\phi}^2 - \frac{P_{,X}}{a^2} (\partial_i \delta\phi)^2 + \cdots \right] \qquad K \equiv P_{,X} + 2XP_{,XX} \qquad c_s^2 = \frac{P_{,X}}{K}$$

For $K > 0$, $c_s^2 < 0$ so gradient instability

For $K < 0$, ghost

No-Go and way-out in a more complex model

Tsujikawa (25)



Modified gravity and dark matter

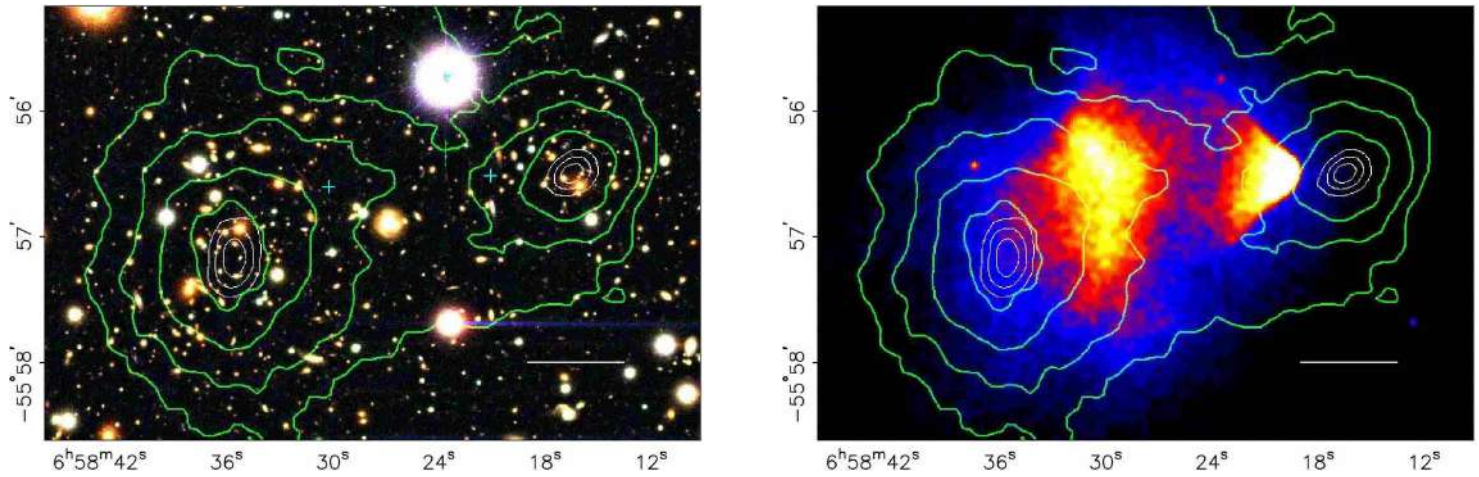


FIG. 1.— Shown above in the top panel is a color image from the Magellan images of the merging cluster 1E0657−558, with the white bar indicating 200 kpc at the distance of the cluster. In the bottom panel is a 500 ks Chandra image of the cluster. Shown in green contours in both panels are the weak lensing κ reconstruction with the outer contour level at $\kappa = 0.16$ and increasing in steps of 0.07. The white contours show the errors on the positions of the κ peaks and correspond to 68.3%, 95.5%, and 99.7% confidence levels. The blue +s show the location of the centers used to measure the masses of the plasma clouds in Table 2.

The mass distribution inferred from gravitational lensing is offset from the hot gas, which dominates the observed baryonic mass.

Clowe et al. (06)

see also Famaey (26)